ANL-6755

Argonne National Laboratory

TWO-COMPONENT TWO-PHASE FLOW PARAMETERS FOR LOW CIRCULATION RATES

by

Georges E. Smissaert

ANL-6755
Engineering and Equipment
(TID-4500, 22nd Ed.)
AEC Research and
Development Report

ARGONNE NATIONAL LABORATORY
9700 South Cass Avenue
Argonne, Illinois 60440

TWO-COMPONENT TWO-PHASE FLOW PARAMETERS FOR LOW CIRCULATION RATES

by

Georges E. Smissaert

Reactor Engineering Division
and
Associated Midwest Universities

July 1963

This report is one of a series that describes heat-transfer and fluid-flow studies performed at Argonne under a program sponsored jointly by the Associated Midwest Universities and the Argonne National Laboratory.

The earlier reports in this series are ANL-6625, ANL-6667, ANL-6674, ANL-6710, ANL-6734, ANL-6738, and ANL-6754.

Reproduced from a Thesis Submitted in Partial Fulfillment of the Requirements for the Degree of Master of Science in Nuclear Engineering in the Graduate School of The Pennsylvania State University.

Operated by The University of Chicago
under
Contract W-31-109-eng-38
with the
U. S. Atomic Energy Commission

TABLE OF CONTENTS

TABLE OF CONTENTS

LIST OF FIGURES

LIST OF FIGURES

LIST OF TABLES

TWO-COMPONENT TWO-PHASE FLOW PARAMETERS FOR LOW CIRCULATION RATES

by

Georges E. Smissaert

ABSTRACT

Two-phase flow parameters for upward cocurrent vertical flow were studied in air-water, nitrogen-Freon-113 and nitrogen-mercury mixtures. Tests were performed in natural-circulation loops at atmospheric pressure. The superficial liquid velocity ranged from 0 to 1 ft/sec; quality ranges were as follows: for air-water, 0.0125 to 0.100; for nitrogen-Freon-113, 0.002 to 0.006; for nitrogen-mercury, 0.00005 to 0.0024. The studies of air-water and nitrogen-Freon-113 mixtures were made in a 2.75-in.-ID test section; the nitrogen-mercury study was made in a 2-in.-ID pipe.

The two-phase flow parameters were found to change significantly with superficial liquid velocity and quality in this low-circulation range. Slip ratios were found to be directly proportional to the surface tension of the liquid, and inversely proportional to the dynamic viscosity of the liquid. Dimensional analysis was used to correlate slip ratios and gas-to-liquid holdups as a function of four dimensionless groups which included the liquid circulation rate, the gas circulation rate, the surface tension of the liquid, the dynamic viscosity of the liquid, the density of the liquid, the density of the gas, the pipe diameter, and the acceleration due to gravity. Empirical relations were developed to evaluate slip ratios and void fractions as a function of the above-listed parameters.

Flow-pattern effects were found to be conveniently described by means of a variable exponent of the Froude number. This exponent was observed to be a linearly decreasing function of the logarithm of the ratio of the volumetric flow rates.

I. INTRODUCTION

A. General Statement of the Problem

Two-phase flow phenomena have been studied for several decades and, although extensive literature is available at the present time, it cannot be said that the fluid flow of a mixture of gas and liquid is completely understood.

The earlier investigations were mainly devoted to practical problems of petroleum and chemical engineering. Moore and Wilde[1] investigated gas slippage occurring in gas-lifts with the purpose of applying the results to oil wells. Peebles and Garber[2] made an extensive study on the motion of gas bubbles in liquid in order to acquire information for the study of such chemical processes as rectification, absorption, and stripping in bubble-cap and perforated-plate contacting devices. The now famous papers by Martinelli, Lockhart, and Nelson[3-5] were the result of two-phase pressure-drop studies which were carried out to assist chemical engineers in the design of boiler tubes, refrigeration systems, and condensate-return lines.

Although a significant amount of work had been done prior to the advent of nuclear power plants, a great deal of additional research was needed to meet the needs of the nuclear industry, particularly for use in the design of boiling-water reactors. Previous correlations were generally confined to specific flow regimes outside the range of need in this new industry. In order to provide the data required, research work on two-phase flow was intensified; the resulting program is still active today, although nuclear power reactors have been built and are operating under conditions often much better than the most optimistic of the early predictions. The EBWR is an outstanding example of a plant whose performance was significantly improved on the basis of new studies on two-phase flow. Originally designed to be operated at 20 Mw, the thermal power of EBWR has been more than tripled because of the better understanding of two-phase flow phenomena.

Despite this progress, there still exist numerous anomalies and gaps in two-phase flow theory. It is known from a previous study by Marchaterre and Hoglund[6] that slip ratio correlations, which are valid for high-circulation flow regions, do not apply to low-circulation regions. Whether or not fluid properties have a significant influence on two-phase flow phenomena is another problem which has not yet been solved. The present work is an experimental study of two-phase flow phenomena in slowly circulating gas-liquid mixtures that provides data and correlations for three different mixtures: air-water, nitrogen-Freon-113, and nitrogen-mercury. A comparison between the results of studies of these three mixtures is provided to help answer the question on the influence of fluid properties.

B. Previous Studies

This section summarizes the nature of the previous work on two-phase flow which is closely related to this study. A summary of the present state of knowledge based on the findings of these authors is presented in Section E of this chapter.

Petrick[7] reported slip velocity ratios in rectangular channels for superficial liquid velocities ranging from 1 to 10 ft/sec as a function of the mixture quality. All experiments were carried out in an air-water mixture at atmospheric pressure. Marchaterre and Petrick[8] reported relative velocities for two-phase mixtures in the following parameter range: pressure, 150 to 2000 $lb_f/in.^2$; mixture quality, 0 to 0.25; superficial liquid velocity, 0.5 to 8 ft/sec; and flow channel equivalent diameters, 0.4 to 2 in. Working curves for the prediction of the velocity ratio in system analyses were given for absolute pressures of 150, 250, 400 and 600 $lb_f/in.^2$. Marchaterre and Hoglund[6] recently published a paper in which all the available results on velocity ratios in steam-water and air-water systems were worked into one correlation which had been proposed by Kutateladze.[9] The authors plotted the velocity ratio against the ratio of the volumetric flow rates, using the Froude number, which is based on the superficial liquid velocity, as a parameter.

Zmola et al.[10] studied the transport of gases through air-water, air-methanol, and air-glycerine mixtures with pipe diameters of 2,6,12 and 24 in. Experimental results were given for circulating and noncirculating systems. Marchaterre et al.[11] reported steam-volume-fraction data from tests performed in natural- and forced-circulation loops, utilizing two different rectangular channels, each 60 in. long, and 0.25 in. by 2 in. in one case and 0.5 in. by 2 in. in the other cross section. The velocity range was from 1 to 6 ft/sec, and the quality range was from 0 to 0.06. Marchaterre[12] also studied the effects of pressure on the boiling density in rectangular channels. Petrick[13] recently reported data on slip ratios in vertical down-flow for pressure ranges up to 1500 $lb_f/in.^2$.

Moore and Wilde[1] carried out a series of experiments to study gas slippage in vertical tubes using water, kerosene, and three different oils. They concluded that the surface tension of the liquid has a definite influence on the slip ratio.

A theoretical model to predict slippage of vapor in a steam-water mixture was proposed by Levy.[14] It is known as the "momentum model" and is based on the assumption that momentum is exchanged between the gaseous and the liquid phases whenever the quality, the void fraction, or

the ratio of the gas density to the liquid density is changed, provided the changes do not occur too rapidly. This exchange of momentum tends to maintain the equality of the combined frictional and head losses of the two phases. Good agreement of the model with available experimental results has been found in many, but not in all, cases. In some of the tests, the changes may have occurred fast enough to cause unbalance between the combined friction and head loss of the two phases; this situation could explain some of the differences between experimental observations and the predictions of this model.

A number of investigators confined their research partly or entirely to the study of the bubble-flow pattern. Petrick[13] studied the bubble-size distribution and the phase distribution in an air-water loop at atmospheric pressure. Siemes[15] made an extensive study of the formation of gas bubbles on single holes and perforated plates. The aperture radius and the volumetric flow rate of the gas were observed to have an influence on the bubble diameters. A second part of his work was devoted to the study of the rise of gas bubbles in liquids with particular attention to the influence of bubble size and fluid properties.

Peebles and Garber[2] studied the flow characteristics of gas bubbles in liquids. Particular attention was paid to the drag coefficient and the steady-state or terminal velocity of the rising bubbles. Zuber and Hench[16] continued the work of the above-mentioned authors by studying the bubble-flow pattern under noncirculating, cocurrent, and countercurrent conditions. Void fractions are reported as a function of the volumetric flow rates of the two phases.

Isbin et al.[17] reported void fractions for annular flow in steam-water mixtures. He investigated vertical flow in a 0.872-in. pipe at atmospheric pressure for qualities from 0 to 0.04 and inlet velocities from 1 to 3 ft/sec. Neal[18] recently reported void fractions in cocurrent nitrogen-mercury flow in a 1-in. pipe. He observed an unstable slug-flow pattern which was due to the nonwetting property of the mercury. Additional data for steam-water mixtures have been obtained by other investigators.[19-27]

C. Definition of Terms to be Used

1. Flow Patterns in Two-phase Flow

Single-phase fluid flow has been recognized to occur either under a laminar or a turbulent type of flow. In most applications, the magnitude of the Reynolds number is sufficient to identify the type of flow. These concepts of laminar and turbulent flow do not disappear in

two-phase flow, but the picture becomes more complicated by the appearance of flow patterns, which are less readily described by one or more mechanical parameters. Based on visual observation, a number of descriptive terms have been established to identify the various flow regimes. These are described below in the order of increasing gas flow rate. Each flow pattern in illustrated in Figure 1.

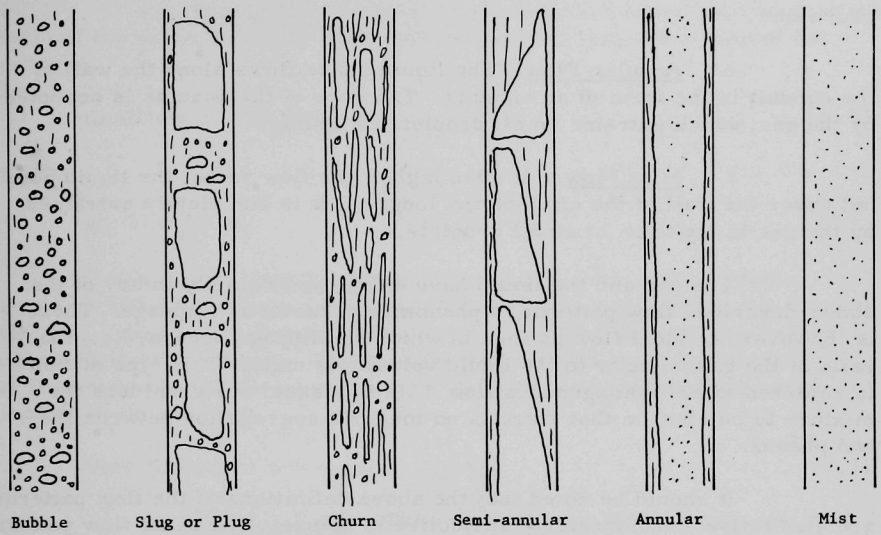

Fig. 1. Vertical Flow Patterns

a. Bubble Flow. The gas phase flows discontinuously in the form of bubbles in a continuous liquid phase. Bubble sizes vary over a narrow range (diameters go from zero to a few centimeters) and their distribution can be described by Poisson's distribution law.[13] The shapes of the bubbles range from spheroids to spherical caps. The bubbles are liable to coalesce and to collapse at random, and have the tendency to crowd toward the center of the channel.

b. Slug or Plug Flow. An increase in the gas flow rate will result in the coalescence of several bubbles, forming large gaseous slugs or plugs. The designation "slug flow" is sometimes reserved for the case in which the liquid phase is flowing continuously. "Plug flow," on the other hand, is used when the gas and the liquid have the tendency to flow alternately.

c. Churn, Froth, or Turbulent Flow. The gas is highly dispersed in the liquid phase, and a strong interaction between the two phases takes place.

d. Semi-annular Flow. This flow pattern is essentially a transition between those described under c and f. It is characterized by the tentative formation of annular flow, which repeatedly collapses into churn flow.

e. Annular Flow. The liquid phase flows along the wall of the conduit in the form of an annulus. The core of the annulus is occupied by the gas, which entrains small droplets of liquid.

f. Mist Flow. At even higher gas flow rates, the liquid does not cover the wall of the channel any longer, but is completely entrained by the gas in the form of small droplets.

The gas and the liquid have a different velocity in any of the above-described flow patterns, a phenomenon known as slippage. There is, however, an ideal flow pattern in which no slippage occurs, i.e., the ratio of the gas velocity to the liquid velocity is unity. This type of flow is referred to as "homogeneous flow." In this case, one considers the mixture to be ideal in that there is no longer a segregation between the two phases.

It should be noted that the above definitions of the flow patterns are qualitative and, therefore, subjective in nature. The same flow patterns are often differently interpreted by various observers. Attempts have been made to avoid this difficulty by more precise definition. Martinelli et al.[3] made a distinction between the various possible flow mechanisms by considering the laminar and turbulent flow possible for both the gaseous and the liquid phases. In this way it was possible to have laminar flow for the gas and turbulent flow for the liquid, or vice versa. It was also possible that the flow of both gas and liquid was either laminar or turbulent. Four flow mechanisms could be identified in that way; the superficial Reynolds number of the phases was taken as the characterizing parameter. This classification of flow mechanisms was successfully used in the analysis of two-phase pressure-drop phenomena; its applicability to other aspects of two-phase flow is not known, however.

Galegar et al.[28] attempted to correlate visually observed flow patterns as a function of the mass velocities of both phases. Correlations of this type, however, show significant discrepancies. More work is needed in this area since present correlations are still largely dependent upon the interpretation of the observers.

2. Parameters in Two-phase Flow

The two-phase flow parameters that will be used in this study are a) the mixture quality, b) the void fraction, c) the slip ratio, d) the relative velocity, e) the superficial liquid velocity, f) the superficial velocity of the mixture, and g) the superficial gas velocity.

a. The Mixture Quality. The mixture quality is defined as the ratio of the mass flow rate of the gas to the total mass flow rate of the mixture:

$$\text{Quality} = X = W_g/W_t \quad , \tag{1.1}$$

where

$$W_t = W_g + W_\ell \quad . \tag{1.2}$$

b. The Void Fraction. The void fraction at a particular cross section is defined as the ratio of the volume occupied by the gas to the total volume of a channel section of unit height which brackets the cross section of interest. The void fraction is also given by the ratio of the cross section through which the gas is flowing to the total cross section of the channel:

$$\text{Void fraction} = \alpha = v_g/v_t = A_g/A_p \quad . \tag{1.3}$$

c. The Slip Ratio. The slip ratio at a particular cross section is defined as the ratio of the actual gas velocity to the actual liquid velocity at the cross section:

$$\text{Slip ratio} = V_g/V_\ell \quad . \tag{1.4}$$

d. The Relative Velocity. The relative velocity at a particular cross section of the channel is defined as the difference between the actual gas velocity and the actual liquid velocity at the cross section:

$$\text{Relative velocity} = V_g - V_\ell \quad . \tag{1.5}$$

e. The Superficial Liquid Velocity. The superficial liquid velocity is understood as the liquid velocity calculated on the basis of the liquid mass flow rate, the liquid density, and the total cross section of the conduit:

$$\text{Superficial liquid velocity} = V_0 = W_\ell/A_p \rho_\ell \quad . \tag{1.6}$$

f. The Superficial Velocity of the Mixture. The superficial velocity of the mixture is defined as the mixture velocity calculated on the basis of the total mass flow rate, the liquid density, and the total cross

section of the channel. This rather strange combination of terms finds its origin in the fact that W_g is generally a much smaller quantity than W_ℓ. The superficial velocity of the mixture is, in most cases, approximated by the superficial liquid velocity. This approximation does not hold for low circulation rates.

$$\text{Superficial velocity of the mixture} = V_{0m} = W_t/A_p\rho_\ell \quad . \tag{1.7}$$

g. The Superficial Gas Velocity. The superficial gas velocity at a particular cross section is defined as the gas velocity calculated on the basis of the mass flow rate of the gas, the total channel cross section, and the density of the gas at the cross section:

$$\text{Superficial gas velocity} = V_{0g} = W_g/\rho_g A_p \quad . \tag{1.8}$$

D. Derivation of Fundamental Equations

The gas and liquid velocities are, by definition, given by the relations

$$V_g = W_g/A_g\rho_g \tag{1.9}$$

and

$$V_\ell = W_\ell/A_\ell\rho_\ell \quad , \tag{1.10}$$

where

$$A_g = \alpha A_p \tag{1.11}$$

and

$$A_\ell = (1-\alpha)A_p \quad . \tag{1.12}$$

The slip ratio is, therefore, equal to

$$\frac{V_g}{V_\ell} = \frac{W_g}{W_\ell}\,\frac{1-\alpha}{\alpha}\,\frac{\rho_\ell}{\rho_g} \quad . \tag{1.13}$$

The ratio of the mass flow rates can also be expressed as

$$\frac{W_g}{W_\ell} = \frac{W_g}{W_t - W_g} = \frac{W_g/W_t}{1 - (W_g/W_t)} = \frac{X}{1-X} \quad , \tag{1.14}$$

and the slip ratio is then determined by

$$\frac{V_g}{V_\ell} = \frac{X}{1-X}\,\frac{1-\alpha}{\alpha}\,\frac{\rho_\ell}{\rho_g} \quad . \tag{1.15}$$

Subtraction of Equation (1.10) from Equation (1.9), and substitution of Equations (1.11) and (1.12) give for the relative velocity:

$$V_g - V_\ell = \frac{W_g}{\alpha A_p \rho_g} - \frac{W_\ell}{(1-\alpha) A_p \rho_\ell} \quad , \tag{1.16}$$

or

$$V_g - V_\ell = W_t \left[\frac{W_g}{W_t} \frac{1}{\alpha A_p \rho_g} - \frac{W_\ell}{W_t} \frac{1}{(1-\alpha) A_p \rho_\ell} \right] \quad . \tag{1.17}$$

Substitution of Equation (1.14) and simplification give

$$V_g - V_\ell = \frac{W_t}{A_p \rho_\ell} \left[\left(\frac{X}{\alpha} \right) \left(\frac{\rho_\ell}{\rho_g} \right) - \left(\frac{1-X}{1-\alpha} \right) \right] \quad . \tag{1.18}$$

Substitition of Equation (1.7) yields

$$V_g - V_\ell = V_{om} \left[\left(\frac{X}{\alpha} \right) \left(\frac{\rho_\ell}{\rho_g} \right) - \left(\frac{1-X}{1-\alpha} \right) \right] \quad . \tag{1.19}$$

E. State of Knowledge on Two-phase Flow Parameters

This section summarizes the state of knowledge based upon the studies outlined in Section B, and the definitions and relationships, identified in Sections C and D. It is known that two-phase flow parameters such as slip, relative velocity, and gas velocity, are dependent upon the flow conditions and the fluid properties. The flow conditions which influence slippage include the quality, the circulation rate, the pressure, and the geometry of the channel. The fluid properties which are believed to have an influence are the gas density, the liquid density, the surface tension of the liquid, and the dynamic viscosity of the liquid. The known effects of these influences are discussed below.

1. Influence of Flow Conditions

As a general rule, the slip ratio and the relative velocity increase with increasing quality. However, the rate of change of the slip as a function of quality is larger for low qualities than for high qualities. The influence of quality on the slip ratio decreases significantly with increasing pressure and also decreases with increasing circulation rate, but to a lesser extent.

Slip ratios decrease and relative velocities increase with increasing superficial liquid velocity. The magnitude of the velocity effect appears to decrease with decreasing quality and increasing pressure. The rate of change of the slip as a function of quality also decreases with increasing circulation rate.

Pressure has a dual influence on two-phase flow phenomena. The increase in gas density, which is a direct effect of the increase in pressure, will reduce the buoyant force which the liquid is exerting on the gaseous phase. As a result, the slip ratio will decrease with increasing pressure. A second effect is the decrease of the volume of gas which is present in the two-phase mixture. This effect results in a change of flow pattern, which has a substantial influence when a churn or semi-annular flow pattern is effective.

Geometry includes such items as the form of the channel cross section (rectangular, circular, etc.) and the magnitude of the equivalent diameter. In general, the geometry effect is only significant for equivalent diameters smaller than 2 in. The effect of geometry is more significant the smaller the equivalent diameter. Flow patterns are believed to be responsible for this phenomenon.

2. Influence of the Fluid Properties

Although previous studies have been successful in establishing an acceptable theory on the effects of flow conditions, the same cannot be said about the understanding of the influence of fluid properties. Although these effects have been studied in the past, there still exist numerous controversies about their relative importance. Fluid properties (density not included) are considered to have little or no influence on slippage. It should be noted, however, that the experimental study of the influence of fluid properties is inherently difficult. There is virtually no way to change one property of a fluid and keep the others constant at the same time. Moreover, in order to investigate a sufficiently wide range, one is compelled to employ different fluids. As a result, the influence of one property is generally masked by that of the other properties.

It is an easily accepted and experimentally verified fact that the slip ratios increase with increasing liquid density. From a previous study by Moore and Wilde[1] it seems that slippage is to some extent dependent upon the surface tension of the liquid. The influence of viscosity has repeatedly been reported as negligible.[1,6,10]

F. Specific Statement of the Problem

The correlation for slip ratios which was proposed by Kutateladze[9] has been worked out by Marchaterre and Hoglund[6] for air-water and steam-water mixtures. The authors plotted the slip ratios as a function of

the ratio of the volumetric flow rates. The Froude number, based on the superficial liquid velocity, was used as the parameter for the family of curves. This correlation by Marchaterre and Hoglund was found to be valid when the superficial liquid velocities were higher than 0.8 ft/sec. Slip ratios for lower superficial velocities were found to deviate significantly from the values predicted by the correlation. Since no reason could be given for this phenomenon, it was concluded that the low circulation range deserved special attention.

This work is a detailed experimental study and evaluation of two-phase flow parameters for superficial liquid velocities ranging from 0 to 1 ft/sec. All experiments were carried out at atmospheric pressure, and the channel diameters were chosen large enough to avoid geometry effects. The quality was extended over as wide a range as permitted by the experimental setup. In order to study the influence of the fluid properties, three different mixtures were used in the experiments: air-water, nitrogen-Freon-113, and nitrogen-mercury.

The parameter ranges in which the tests, all at a pressure of one atmosphere, were carried out are listed in Table I. The fluid properties of the three liquids are given in Table II.

Table I

PARAMETER RANGES

Mixture	Quality Range	Channel Diameter (in.)	Superficial Liquid Velocity (ft/sec)
Air-Water	0-0.10	2.75	0-1
Nitrogen-Freon-113	0-0.02	2.75	0-1
Nitrogen-Mercury	0-0.0024	2.00	0-1

Table II

FLUID PROPERTIES AT ROOM TEMPERATURE

Liquid	Specific Gravity	Viscosity (lb_m/ft-sec x 10^{-3})	Surface Tension (dynes/cm)
Water	1.0	0.7	73
Freon-113	1.55	0.415	19
Mercury	13.6	1.0	487

II. EXPERIMENTAL APPARATUS

All experiments were performed in natural-circulation loops. The air-water and nitrogen-Freon mixtures were tested in the same loop, which is schematically depicted in Figure 2; details of the test section are given in Figure 3. The loop was modified for the study of the nitrogen-mercury mixture. A schematic drawing of this modified loop is given in Figure 4, and details of the nitrogen-mercury test section are given in Figure 5.

The loops consisted of two vertical legs known as the riser and downcomer, respectively, which were connected at the top to a vented separator tank; a horizontal pipe made the connection at the bottom. The gas and the liquid were mixed in a special mixer sleeve at the bottom of the riser, which is shown on the right of Figures 2 and 4. The lower part of the riser was used as a stabilizing zone to neutralize all entrance effects. The upper part of the riser was used as the actual test section, and was equipped with the measuring apparatus for the determination of the void fraction and the absolute pressure at the test points. The gas was separated from the liquid in a Lucite separator tank at the top of the loop and was evacuated through a vent. The liquid was recirculated through the downcomer, which is shown on the left of Figures 2 and 4.

The liquid was introduced into the loop through a supply line at the bottom of the downcomer. The liquid circulation rate was measured by means of an orifice flow meter installed in the horizontal section which connects downcomer and riser. A bimetal dial thermometer was used to measure the temperature of the liquid. The liquid circulation rate was controlled by means of a bypass control line in the downcomer. The gas flow rate was measured by means of an orifice flow meter, and was controlled by means of a pressure regulator upstream of the orifice and a bypass control line downstream of the orifice. This bypass line gave access to the gas-liquid mixer at the bottom of the riser. Detailed description of specific features of each loop is given below.

A. The Air-Water and Nitrogen-Freon Loop

The air-water experiments were made with regular tap water, which was changed when the loop had to be emptied for changing the orifice plate in the liquid flow meter. The Freon-113 which was used in the nitrogen-Freon experiments was saved whenever it had to be drained from the loop. Make-up Freon was added at regular intervals in order to compensate for the high evaporation rate.

The air for the air-water experiments was supplied by the laboratory 100-psi compressed-air line. The nitrogen for the nitrogen-Freon experiments was supplied by a battery of four gas cylinders. A pressure regulator was used to keep a constant gauge pressure of 25 $lb_f/in.^2$ upstream of the

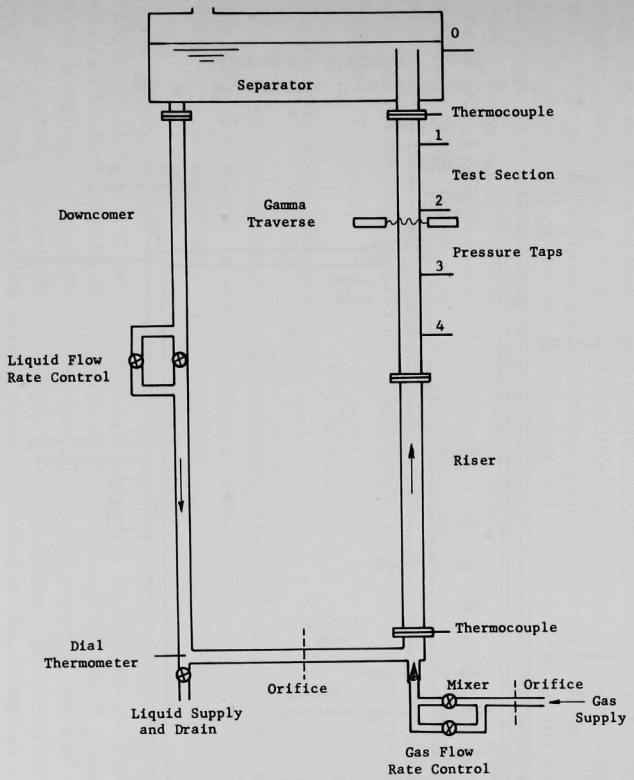

Fig. 2. Schematic Representation of Air-Water and Nitrogen-Freon Loop

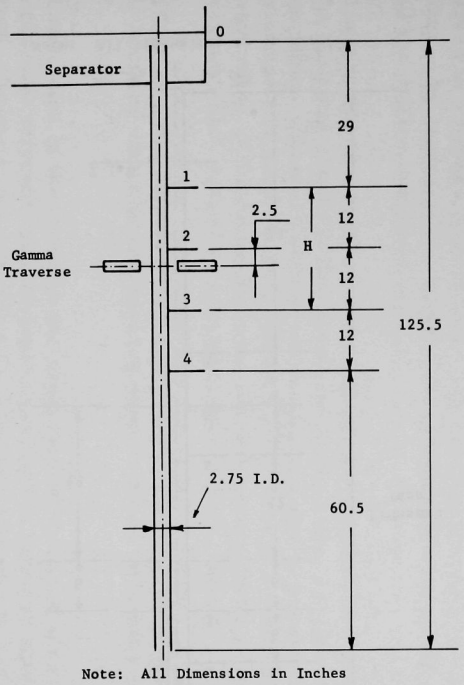

Fig. 3. Air-Water and Nitrogen-Freon Test Section

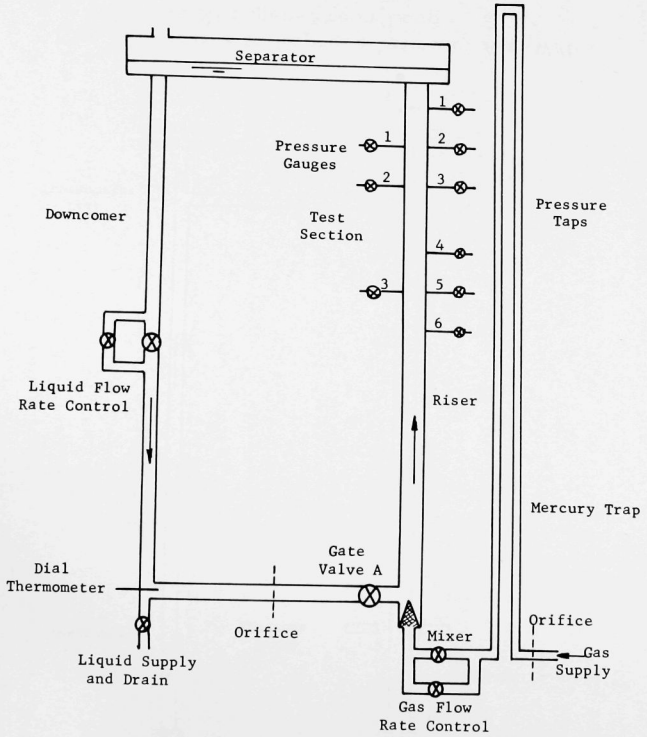

Fig. 4. Schematic Representation of Nitrogen-Mercury Loop

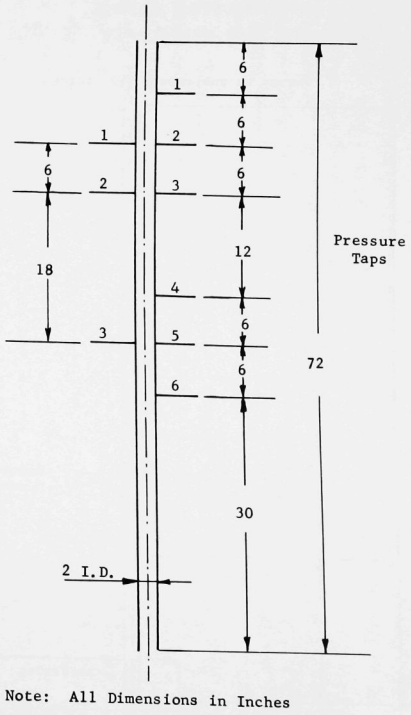

Fig. 5. Nitrogen-Mercury Test Section

orifice of the gas flow meter. The gas flow rate was controlled by means of two valves in a bypass control line. The gas temperature at the orifice was measured by means of two bimetal dial thermometers up and downstream of the orifice, respectively.

The gas-liquid mixer was constructed from a pipe tee. The gas entered at the bottom and the liquid entered at the side. The gas was passed through a 150-mesh screen which was intended to provide a uniform gas distribution and bubble size at the entrance of the test section. The screen was rolled in the form of a cone and was covered with a heavier conical screen which served as a support for the light screen.

The riser was a 2.75-in.-ID Lucite pipe, 124.5 in. long, made from two equal sections which were glued together in order to provide a perfect joint.

The motion of the liquid in the separator tank caused pressure pulses which might have affected the instrument readings if they had entered the test section. To avoid this difficulty, the pipe was extended 9.5 in. into the separator tank. The liquid level in the separator tank was kept one inch above the top of the pipe. The lower 5 ft of the riser was used as a stabilizing zone in order to obtain flow patterns which were not affected by entrance effects. The upper 5 ft was then considered as the actual test section in which four pressure taps were mounted (see Figure 3). A fifth tap was arranged at the wall of the separator tank at the same level as the edge of the pipe. Differential manometers were used to measure pressure differences between the taps Nos. 0 and 1, 1 and 3, and 2 and 4. The centerline of the gamma traversing equipment, i.e., the centerline of the source pellet and the scintillation detector, was 2.5 in. lower than the centerline of tap No. 2. Thermocouples were installed at the top and the bottom of the riser to determine the average temperature of the two-phase mixture in the test section.

B. The Nitrogen-Mercury Loop

The design of the nitrogen-mercury loop was influenced largely by the steps that had to be taken to assure wetting of the test section by the mercury. These features are identified in the description presented below.

The mercury was contained in a hermetically sealed stainless steel cylinder which was about one foot high and 10 in. in diameter. The liquid was introduced into the loop by pressurizing the cylinder to a gauge pressure of 80 $lb_f/in.^2$ After the loop was filled with mercury and the valve in the connecting line between container and loop closed, the pressure was released by opening a small needle valve at the top of the container. This valve was kept open during operation of the loop; in that way, it was possible to drain the mercury at once in the event of a failure of a part of the loop.

The nitrogen was supplied by a battery of four gas cylinders and passed through a gas filter, a flow meter, a mercury trap, and a bypass control line, respectively, before entering the gas-liquid mixer. The mercury trap was installed between the bypass control line and the orifice flow meter in order to prevent any mercury from being deposited in the flow meter pipe.

A constant gauge pressure of 70 lbf/in.^{2} was kept upstream of the orifice flow meter during operation of the loop. The gas-liquid mixer was the same as the one used for the air-water and the nitrogen-Freon experiments.

The riser for the nitrogen-mercury loop was a 6-ft high, 2-in.ID nickel-plated pipe. In the choice of the test section special attention was paid to the fact that mercury is a nonwetting liquid to almost all surfaces. Although the experiments could have been performed in a nonwetted test section, there existed several reasons for preferring a pipe in which the liquid presented a high degree of adhesion to the wall.

Earlier observations[18] of gas rising through mercury in a glass pipe revealed that the gas had a tendency to rise along the wall of the pipe. The liquid-wall interface was a path of least resistance because of the nonwetting properties of the mercury. When tests were performed with liquids which did wet the pipe wall, however, it was observed that the gaseous phase was concentrated at the center of the conduit. The existence of a preferential path along the pipe wall has been reported to cause an unstable flow pattern which is accompanied by severe static pressure oscillations.[18] It was intended to compare the results of the nitrogen-mercury study with those obtained for the other mixtures. A comparison, however, could be justified only if the flow patterns in the nitrogen-mercury flow were similar to those which occurred in the other mixtures. A mercury-wetted pipe wall was therefore necessary.

Mercury-wetted surfaces are commonly obtained by adding wetting agents to the liquid metal. The addition of 0.1 per cent sodium, or 0.02 per cent magnesium together with 0.0001 per cent titanium, which serves to reduce the corrosive properties of the mercury, was successfully applied in the past whenever high temperatures were involved.[29-31] This technique, however, was found to fail at room temperature. An attempt was made to obtain a mercury-wetted surface by using a clean liquid and a clean, smooth surface. Tests performed with possible surface materials showed that a nickel surface was wetted by mercury at room temperature after it had been treated by dilute hydrochloric acid. It was further observed that the best results were obtained when the nickel surface had not been given time to dry after it had been exposed to the acid solution. Rubbing the submerged surface by a brush or shaking the sample piece in the liquid was found to promote wetting. It was also observed that the surface remained

wetted by the mercury as long as the submersion was not discontinued for too long a time. A prolonged exposure of the wetted surface to the air resulted in the formation of oxides which inhibited further wetting. The oxides were found to be formed in a period of the order of one hour.

Based on these observations, the test section was plated with a 0.002-in. nickel coating. In order to avoid the formation of oxides it was necessary to keep the mercury in the test section during the entire experimental program. It was, therefore, necessary to build the test section in such a way that it could be closed off from any other part of the loop or the measuring apparatus. The bottom of the riser could be blocked off by the valves in the bypass lines of the gas inlet, and by a gate valve (designated as "A" in Figure 4) installed at the end of the horizontal connection between downcomer and riser. In order to provide flexibility for varying the distance across which the pressure differences were to be measured, the test section was built with a larger number of pressure taps than actually needed. Some trial runs would then be made to determine what combination of pressure taps would give satisfactory precision. As a result, six pressure taps were installed at the test section for connection to differential manometers. In addition, three taps were provided for connection to pressure gauges. When adequately combined, the taps could form test sections which were either 6, 12, or 24 in. long. All taps were provided with needle valves so that changes could be made after the loop had been filled.

The following procedure was used to obtain a mercury-wetted test section. The riser was completely closed off from the rest of the loop, and the separator was removed. A solution of 50 per cent hydrochloric acid was poured into the riser from the top, and the mercury was introduced as soon as the riser was filled with acid solution. The remaining part of the loop was filled with mercury after the separator had been installed, the gate valve "A" was opened, and nitrogen was blown through the mercury for about 15 min. This procedure permitted the wetting process to be promoted by the turbulent two-phase flow. The above-described procedure led to a test section which was later observed to have been wetted by mercury over more than ninety per cent of its inner surface. This fact was determined by detailed examination of the surface after the loop had been drained.

C. Instrumentation

The parameters that were to be measured during operation of the loops were the following: the void fraction at the test point, the absolute pressure at the test point, the liquid flow rate, the gas flow rate, and the temperature of the fluids.

The void fractions were obtained primarily from differential pressure measurements between two points. A number of gamma traverses were made to check results obtained with the foregoing method. The gamma

traversing system, however, had a number of inherent inaccuracies which made the data less self-consistent than the data from the pressure-difference measurements. In addition, the use of the gamma traversing system was time-consuming for routine work. Absolute pressures were determined by adding differential pressure readings. This technique was not used for the nitrogen-mercury experiments, for which pressure gauges were found to be more convenient and to give sufficient precision. Liquid and gas flow rates were measured with orifice flow meters. Temperatures were obtained from thermocouple or bimetal dial thermometer readings.

1. The Gamma Traversing Equipment

The principle of the gamma traversing equipment is based on the fact that the attenuation of gamma rays in matter is proportional to the density of the material on which the gamma rays impinge. A collimated gamma beam traverses the channel in a plane which is perpendicular to the channel axis. Traverses are made when the channel is empty, full, and filled with two-phase mixture, respectively. The void fraction in the two-phase mixture is then readily determined from a comparison between the attenuation obtained in each of these three conditions. This method has been described and discussed several times before;[7,32] as a result, only a short review of the experimental setup and the operation is given below. A typical setup of this void-measuring apparatus is given in Figure 6.

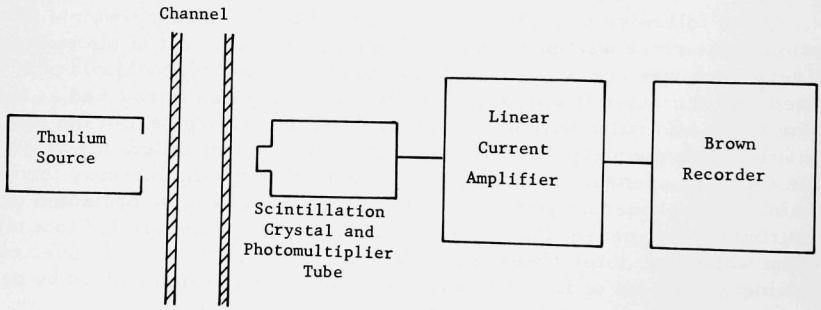

Fig. 6. Void-measuring Apparatus

The gamma source was a thulium-170 pellet, enclosed in an aluminum container. Thulium-170 has a half-life of 129 days, and its energy spectrum shows peaks at 0.053 Mev and at 0.084 Mev. The 0.053-Mev peak was absorbed by inserting a lead plate (0.0625 in. thick) between the source and the channel in order to obtain the required monoenergetic radiation. At the time of the tests, the thulium pellet produced a dose rate of 2 r/hr at a distance of 2.5 in. after its low-energy peak had been absorbed by the lead plate.

The detector was a NaI(Tl) scintillation crystal optically coupled by a Lucite light pipe to a Dumont photomultiplier tube. The gamma beam was collimated by a rectangular window (0.03 in. by 0.5 in. in cross section) which was cut in the face of the 1-in.-thick lead shield that surrounded the crystal. Cooling coils in the shield kept the temperature constant within ±0.5°F. This cooling was necessary since the functioning of both the scintillation crystal and the photomultiplier tube was temperature sensitive. The supply voltage to the photomultiplier tube could be regulated to within 0.1 per cent of the scale reading. The unattenuated gammas produced a signal in the photomultiplier which was then amplified before being transmitted to a Brown recorder of 0 to 10-mv range. Changes in source strength were corrected by taking full and empty channel traverses twice daily. Amplifier-drift errors were reduced by taking full channel traverses every three or four runs. The average error in the determination of void fractions by the gamma traversing equipment was of the order of seven per cent. The precision of this technique, however, decreased significantly with decreasing values of the void fractions.

2. Manometers

All manometers were mounted for differential pressure measurements. Indicating fluids had specific gravities of 1.75, 2.95, and 13.6, respectively. The scale range of each manometer was 60 in., and the scales were graduated in inches and tenths of inches.

The manometers which were used to determine void fractions in the nitrogen-mercury mixture deserve special mention. The continuous collapse of the two-phase flow structure in the test section resulted in heavy pulsations in the manometer legs; this was particularly serious for static pressure taps. Differential manometers, however, damped the pulsations to an extent that sufficient precision and reproducibility of the data could be obtained. The principle of differential manometers was applied to this mercury flow system by inverting U-tube manometers so that the connection to the test section could be made at the bottom of the manometers. Both legs were connected by a water column on top of the mercury.

A second problem in the construction of the manometer system originated from the requirement of having short distances between the pressure taps at the test section. Long distances would give more precise readings on the manometers. Short distances, however, were preferred in order to reduce the error in the determination of the gas density which corresponded to the average void fraction between two pressure taps. The test point was considered to be at halfway the distance between the two taps. The gas density at that point was determined from gauge pressure measurements. This procedure could not be justified unless the pressure variation between the two manometer taps could be approximated by a straight line; this required short distances between the taps. The problem was successfully solved by inclining the manometers to 10° with the horizontal. A schematic representation of this manometer system is shown in Figure 7.

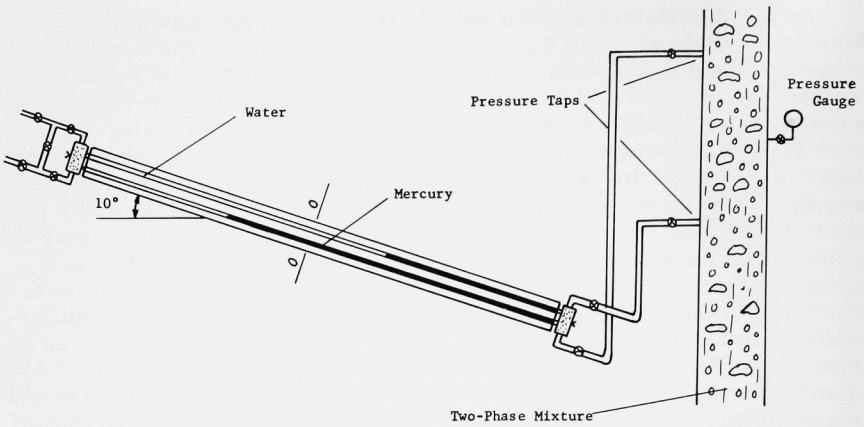

Fig. 7. Inclined Manometer for Void-fraction Determination in the Nitrogen-Mercury Mixture

3. Orifice Flow Meters

Both gas and liquid flow rates were measured by means of orifice flow meters which were constructed according to the recommendations of Grace and Lapple.[33] The liquid flow rate was measured in a 1.5-in.-ID pipe; the orifice plates were 0.500, 0.750 and 1 in. in diameter, respectively. The gas flow meter line was a 1-in.-ID pipe and the orifice diameters were 0.0312, 0.0597, 0.1250, and 0.5000 in., respectively. All orifice diameters had a maximum uncertainty of ±0.0005 in.

4. Pressure Gauges

The absolute pressure at the test points in the nitrogen-mercury mixture was measured by means of Ashcroft pressure gauges with a maximum scale reading of 30 $lbf/in.^2$. The precision of the gauges was ±1 per cent of the maximum scale reading.

5. Dial Thermometers and Thermocouples

Bimetal dial thermometers were used to measure the average temperature of the gas at the orifice flow meter and to determine the temperature of the liquid at a point upstream of the liquid orifice flow meter. The precision of these thermometers was ±1°C. Iron-constantan thermocouples were used to determine the average temperature of the two-phase mixture in the test section. The voltages were measured by means of a Rubicon potentiometer. The temperatures could be measured with a precision of ±1°F.

III. EXPERIMENTAL PROCEDURES

The procedure which was followed throughout the experimental program is summarized below. After the loop was filled with liquid and the manometer lines cleared of bubbles, the gas flow was started and the liquid circulation was adjusted to the desired rate. The following variables were then recorded: the liquid flow rate, the gas flow rate, the average temperature of the two-phase mixture, the barometric pressure, and the pressure differences between the taps on the test section. For a specific circulation rate of the liquid, the gas flow rate was varied over as wide a range as permitted by the experimental setup. In that way it was possible to determine how a two-phase flow parameter (e.g., the slip ratio) was varying as a function of quality. This completed, the liquid circulation rate was adjusted to another value and a new series of tests was started. Two-phase flow parameters were determined as a function of quality for superficial liquid velocities of 0, 0.1, 0.2, 0.3, 0.4, 0.6, 0.8, and 1 ft/sec, respectively.

The results, which are presented in Chapter IV for air-water and nitrogen-Freon mixtures, were derived from data obtained at test point No. 2 (see Figure 2). The data for the nitrogen-mercury mixture were obtained at test point No. 5 (see Figure 5).

Inasmuch as [see Equation (1.15)],

$$\frac{V_g}{V_\ell} = \left(\frac{X}{1-X}\right)\left(\frac{1-\alpha}{\alpha}\right)\left(\frac{\rho_\ell}{\rho_g}\right) \quad , \tag{1.15}$$

the determination of the slip ratio required the measurement of the quality X, the void fraction α, the gas density ρ_g, and the liquid density ρ_ℓ. The other two-phase flow parameters were derived from the same data. The quality was determined by the ratio of the gas flow rate to the total mass flow rate. The gas and liquid flow rates were measured by means of orifice flow meters, and the calculations were carried out according to the recommendations of Grace and Lapple.[33] The void fraction was determined from pressure-drop measurements or by means of the gamma traversing equipment. The determination of the gas density consisted essentially in the measurement of the absolute pressure at the test point. The exact liquid density was derived from temperature measurements obtained by means of a bimetal dial thermometer. The experimental procedure was the same for the three mixtures. The reduction of the data, however, was slightly different for each mixture and is described below.

A. Reduction of the Air-Water Data

The void fraction and the absolute pressure at the test point were derived from pressure-drop measurements. The reduction of the data was based on the following theory.

Consider a vertical channel in which a two-phase mixture is flowing at a steady rate. The pressure drop ΔP between two points can be written as

$$\Delta P = \Delta P_h + \Delta P_{tpf} + \Delta P_{ac} \quad , \tag{3.1}$$

being given by the sum of the hydrostatic head ΔP_h, the frictional pressure drop ΔP_{tpf}, and the acceleration pressure drop ΔP_{ac}. The frictional pressure drop is evaluated by the relation

$$\Delta P_{tpf} = R\Delta P_\ell = R\left(4f \frac{H}{D} \frac{\rho_\ell V_0^2}{2g_c}\right) \quad , \tag{3.2}$$

where R is the Martinelli-Nelson friction factor and f the Fanning friction factor for single-phase flow. The low superficial liquid velocity ($V_0 \leq 1$ ft/sec), however, does not cause a significant frictional pressure drop, the maximum value of the term ΔP_{tpf} being 2 per cent of the hydrostatic head ΔP_h. Thus, the frictional pressure drop can be neglected with respect to the hydrostatic head.

The maximum value of the acceleration pressure drop is obtained from homogeneous flow theory. If it be assumed that a homogeneous mixture flows in the test section (see Figure 2), the rate of change of momentum between the points 1 and 3 can be written as

$$A_p \Delta P_{ac} = \frac{W_t}{g_c} (V_1 - V_3) \quad , \tag{3.3}$$

V_1 and V_3 being the velocity of the two-phase mixture at the positions 1 and 3, respectively. We also have

$$W_t/A_p = G \quad ; \tag{3.4}$$

$$V_3 \bar{\rho}_3 = V_1 \bar{\rho}_1 = G \quad ; \tag{3.5}$$

and

$$\bar{\rho} = (1 - \alpha)\rho_\ell + \alpha\rho_g \cong (1 - \alpha)\rho_\ell \tag{3.6}$$

unless $\alpha \cong 1$. Substitution of Equations (3.4) to (3.6) into Equation (3.3), followed by rearrangement, yields

$$\Delta P_{ac} = \frac{G^2}{g_c \rho_\ell} \left[\frac{1}{1 - \alpha_1} - \frac{1}{1 - \alpha_3}\right] \quad , \tag{3.7}$$

or

$$\Delta P_{ac} = \frac{G^2}{g_c \rho_\ell} \left[\frac{\alpha_1 - \alpha_3}{(1 - \alpha_1)(1 - \alpha_3)}\right] \quad . \tag{3.8}$$

The mass flow rate per unit area, G, is small because of the low superficial velocities which are involved. The maximum value of the acceleration pressure drop is found to be of the order of 1 per cent of the value of the hydrostatic head. Thus, the term ΔP_{ac} can be neglected, and Equation (3.1) becomes

$$\Delta P = \Delta P_h = H\left[(1-\bar{\alpha})\rho_\ell + \bar{\alpha}\rho_g\right] = H\rho_\ell(1-\bar{\alpha}) \quad , \tag{3.9}$$

H being the distance between two pressure taps. The average void fraction between two taps is now given by the formula

$$\bar{\alpha} = 1 - \frac{\Delta P_h}{H\rho_\ell} \quad . \tag{3.10}$$

The absolute pressure at the test point was determined by adding $\Delta P_{01} + \frac{1}{2}\Delta P_{13}$ to the barometric pressure (see Figure 2). This procedure was acceptable for the air-water mixture, since the pressure variation as a function of channel height could be approximated by a straight line.

B. Reduction of the Nitrogen-Freon Data

The experimental study of the nitrogen-Freon mixture was the most difficult of the studies made because of secondary effects. These effects included mixing of the Freon with the indicating fluids in the manometer legs, evaporation of the Freon into the nitrogen, severe temperature changes as a result of this vaporization, and finally a serious loss of expensive liquid, which limited the amount of data that could be taken. As a result, the superficial liquid velocities had inaccuracies of ±10 per cent. In addition, because of the mixing of the manometer fluid with the Freon, void fractions determined by pressure-drop measurements were in question. Therefore, the void fractions had to be determined by the gamma traversing technique. Furthermore, the slip-quality relations became dependent upon the relative humidity ϕ of the gas phase.

The evaporation of Freon into the nitrogen resulted in a change of the density of the gas phase. It can be shown, however, that the void fraction at a point in the riser did not depend upon the density of the gas phase. The driving force in the natural-circulation loop originated from the presence of a two-phase mixture in the riser and corresponded to

$$F = A_p \Delta P_t = A_p \Delta P_h = A_p H\rho_\ell(1-\bar{\alpha}) \quad , \tag{3.11}$$

with

$$\bar{\alpha} = \frac{\int_0^H \alpha(H)\, dH}{H} \quad . \tag{3.12}$$

The natural-circulation loop was operated in such a way that a constant circulation rate was maintained during a run. This implied that the driving force was constant. Equation (3.11) shows that this condition was equivalent to the condition of a constant average void fraction in the riser. It is left to prove that the variation of the void fraction $\alpha(H)$ as a function of channel height was not affected by the change in composition of the gaseous phase. It is sufficient to show that the evaporation of the Freon did not result in a substantial change of the compressibility factor C of the gas phase. The compressibility factor of the nitrogen was 0.998. The compressibility factor of the Freon vapor was derived from a comparison between its Beattie-Bridgman equation of state[34] and the ideal gas law. It was found to vary between 0.994 and 0.981 in the temperature and pressure ranges that were pertinent to these experiments. Thus, the gas mixture could be treated as an ideal gas for any value of the relative humidity ϕ. Therefore, the variation of the void fraction with channel height was independent of the relative humidity. As a result, the knowledge of the void fraction for one value of ϕ, although unknown, could be used in the calculation of the slip ratios for any value of ϕ.

The absolute pressure at the test point was determined by an iteration calculation which was based on the relation

$$\Delta P_h = \rho_\ell (1 - \overline{\alpha}) H \quad . \tag{3.9}$$

Further reduction of the data was performed as follows.

The saturation pressure P_{sat} of the Freon vapor depended only upon the temperature existing at the test point. The partial pressure P_s of the Freon vapor was given by

$$P_s = \phi P_{sat} \quad , \tag{3.13}$$

and the partial pressure of the nitrogen gas was then given by

$$P_{N_2} = P - P_s \quad , \tag{3.14}$$

the absolute pressure at the test point being denoted by P. The specific volume of the nitrogen was then readily determined from Equation (3.14) as

$$v_{N_2} = R_{N_2} T / P_{N_2} \quad , \tag{3.15}$$

R_{N_2} being the ideal gas constant of the nitrogen, and T the absolute temperature at the test point. The specific humidity SH was defined as the number of pounds of Freon vapor per pound of dry nitrogen and was given by

$$SH = \phi \frac{v_{N_2}}{v_{gFR}} \quad , \tag{3.16}$$

v_{gFR} being the specific volume of the Freon vapor. The mass flow rate of the Freon vapor at the test point was then equal to

$$W_{gFR} = SH\ W_g = SH\ W_{N2} \quad , \tag{3.17}$$

and the quality was given by

$$X = \frac{W_{gFR} + W_{N2}}{W_t} \quad . \tag{3.18}$$

The density of the gas phase was determined by the relation

$$\rho_g = \rho_{N2} \frac{(1+SH)}{\left(1 + SH \frac{M_{N2}}{M_{FR}}\right)} \quad , \tag{3.19}$$

with M_{N2} and M_{FR} denoting the molecular weights of nitrogen and Freon-113, respectively.

C. Reduction of the Nitrogen-Mercury Data

The reduction of the nitrogen-mercury data was similar to the reduction of the air-water data. The approximations

$$\Delta P_{tpf}/\Delta P_h \simeq 0 \quad ; \quad \Delta P_{ac}/\Delta P_h \simeq 0$$

could not be verified by means of gamma traverses. They were believed to be valid, however, because the void fractions never exceeded the value 0.500. This implied low frictional and acceleration pressure drops. As a result, the void fraction was readily determined by means of Equation (3.10):

$$\bar{\alpha} = 1 - \frac{\Delta P_h}{H \rho_\ell} \quad . \tag{3.10}$$

The absolute pressure at the test point was determined by means of pressure gauges.

IV. EXPERIMENTAL RESULTS

This chapter presents the experimental results of the three mixtures in graphical form. The results are discussed in detail, and a short error analysis is given to emphasize the precision of the experimental procedure.

A. Presentation and Discussion of Results

Results are presented for superficial liquid velocities of 0.1, 0.2, 0.3, 0.6, and 1 ft/sec. The results for the superficial velocities of 0.4 and 0.8 ft/sec have been omitted for the sake of clarity in the graphical presentation; they fell within the bounds set by the results for 0.3 and 0.6 ft/sec, and 0.6 and 1 ft/sec, respectively.

The slip-velocity ratios of the air-water mixtures are presented as a function of quality and circulation rate in Figure 8. A similar plot is given for the nitrogen-mercury slip ratios in Figure 9. It can be seen that the slip ratios increase with quality, and decrease with circulation rate. The influence of the circulation rate, however, decreases with increasing superficial liquid velocity. The results of the nitrogen-mercury study clearly illustrate that the influence of the circulation rate also decreases with decreasing quality. It is finally noted that the slopes of the slip-quality lines decrease with increasing quality. The above observations are consistent with those obtained in previous studies (see Section E of the Introduction).

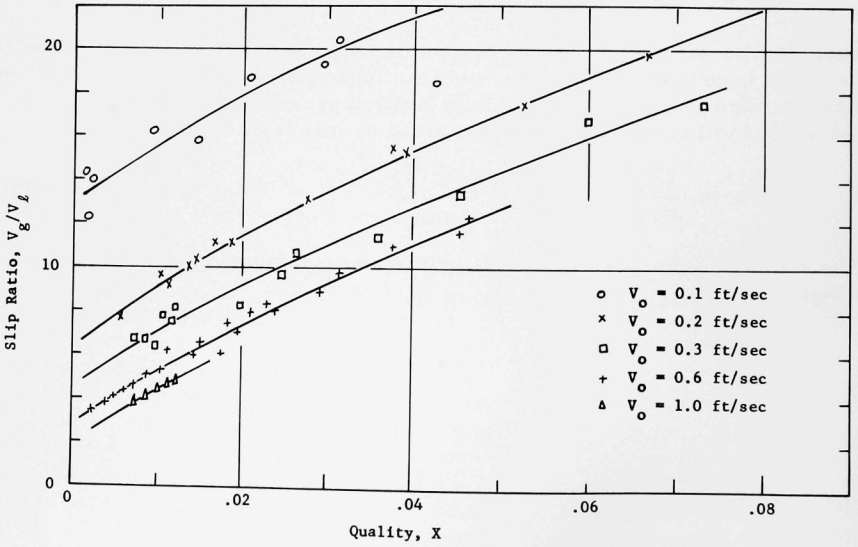

Fig. 8. Slip Ratio as a Function of Quality and Superficial Liquid Velocity for the Air-Water Mixture

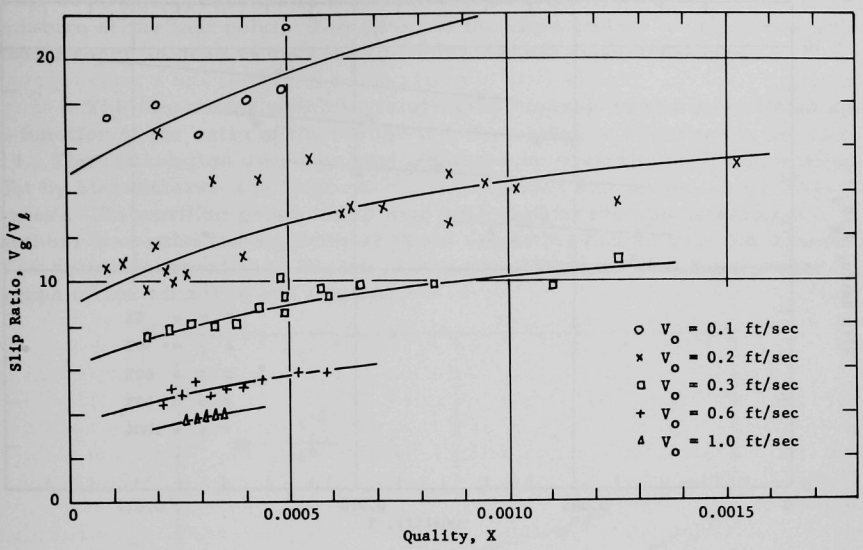

Fig. 9. Slip Ratio as a Function of Quality and Superficial Liquid Velocity for the Nitrogen-Mercury Mixture

The nitrogen-mercury slip ratios determined in this study were significantly higher than those which Neal[18] obtained in a 1-in.-ID nonwetted test section. An acceptable explanation for the significant difference in the slip ratios is based on the fact that the nonwetting property of the mercury in Neal's test section caused the formation of large gas slugs. Neal reported that these slugs were rising along one side of the channel wall, while the mercury was flowing downwards along the opposite side of the wall. Neal's visual study of flow in a 1-in.-ID nonwetted glass pipe revealed slugs of lengths up to 8 in. The velocity of a slug of that size was apt to be strongly affected by the size of the conduit. The nitrogen-mercury tests of this study, however, were performed in a wetted 2-in.-ID nickel-plated test section. Because the pipe was wetted it is believed that the formation of large slugs was not encountered in the present tests. This difference in flow conditions possibly explains the difference in the slip ratios.

Figures 10 and 11 give slip ratios in a nitrogen-Freon mixture as a function of quality and relative humidity of the gas phase for two specific circulation rates. It is recalled that the Freon evaporated into the nitrogen. As a result, the gas phase was a mixture of nitrogen and Freon vapor. The relative humidity ϕ of the gas phase is the ratio of the partial pressure of the Freon vapor in the gas phase to the saturation pressure of the Freon.

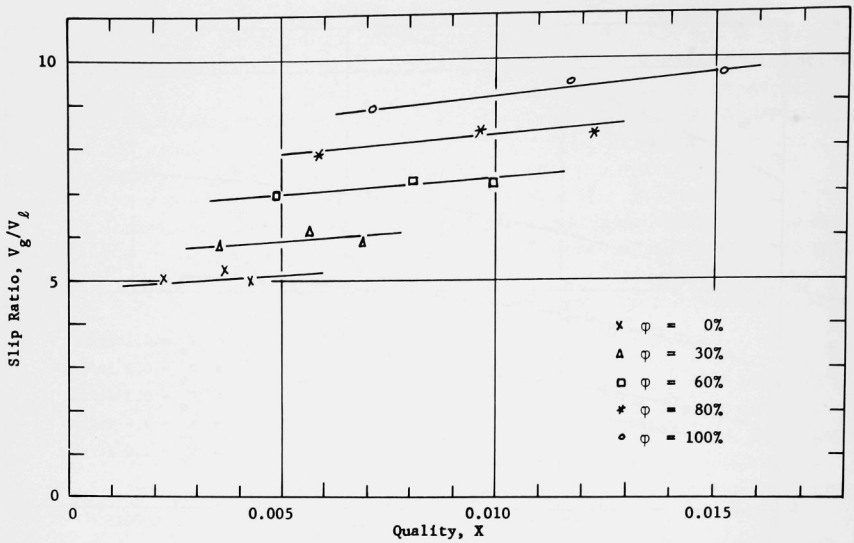

Fig. 10. Slip Ratio as a Function of Quality and Relative Humidity of the Gas Phase for the Nitrogen-Freon-113 Mixture for V_0 = 0.36 ft/sec

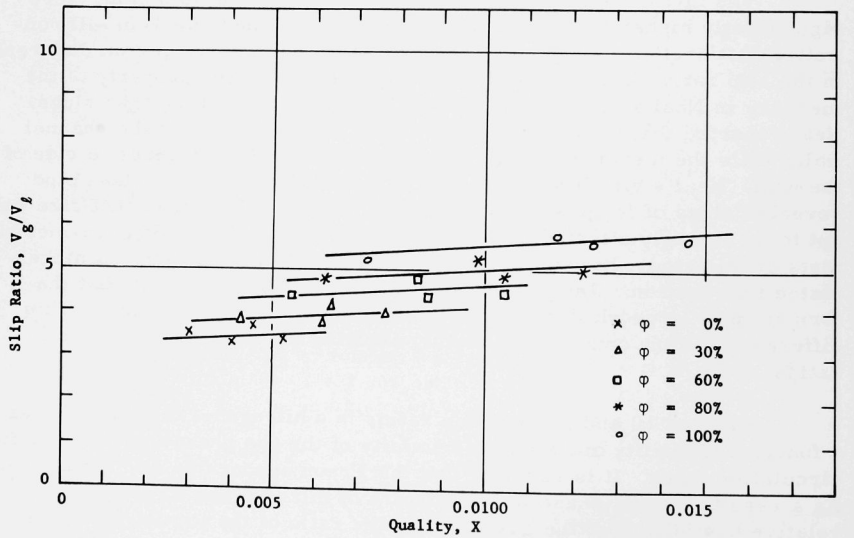

Fig. 11. Slip Ratio as a Function of Quality and Relative Humidity of the Gas Phase for the Nitrogen-Freon-113 Mixture for V_0 = 0.87 ft/sec

This saturation pressure is a function of the temperature of the two-phase mixture at the test point. The effect of the vaporization of the Freon into the nitrogen is seen to decrease with increasing circulation rate.

The slip ratios which were given in Figures 8 to 11 are plotted as a function of the ratio of the volumetric flow rates in Figures 12, 13, and 14. The correlation used was that proposed by Kutateladze[9] and worked out by Marchaterre and Hoglund[6] for air-water and steam-water mixtures. The working graph which was published by the aforementioned authors was valid for superficial liquid velocities higher than 0.8 ft/sec. The results presented in Figure 12 are not consistent with the working graph of Marchaterre and Hoglund.

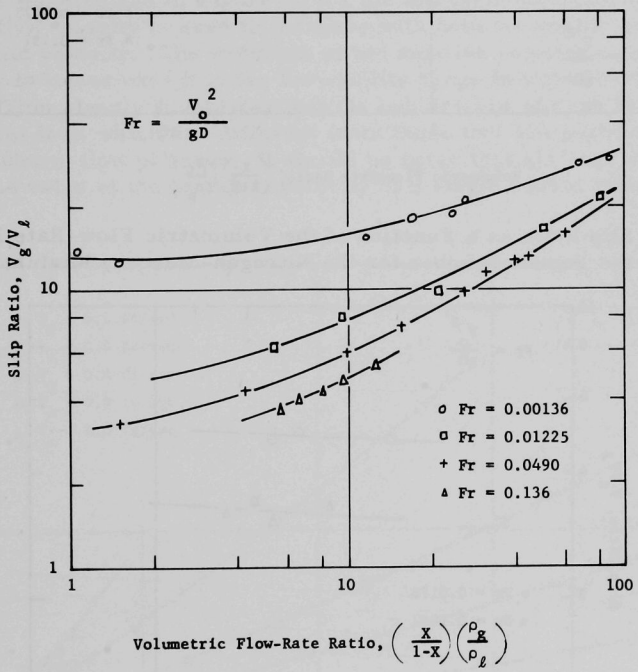

Fig. 12. Slip Ratio as a Function of the Volumetric Flow-Rate Ratio and the Froude Number for the Air-Water Mixture

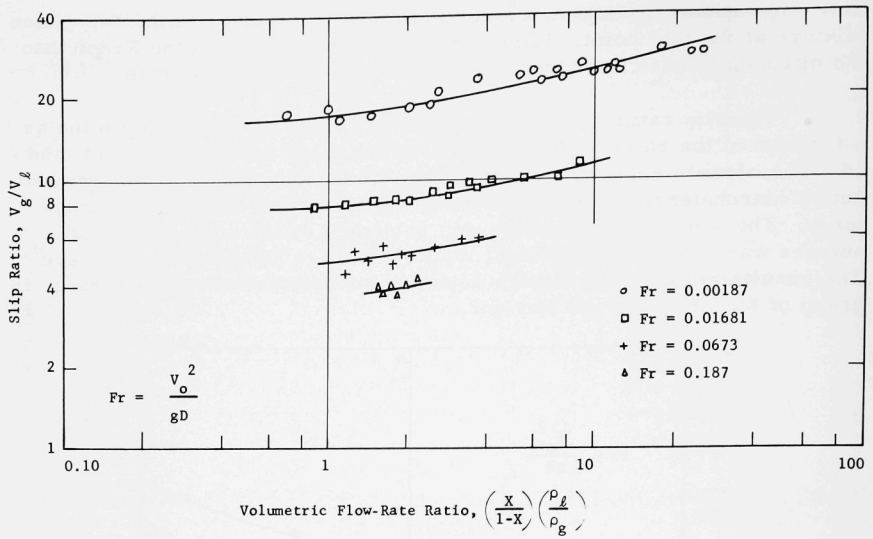

Fig. 13. Slip Ratio as a Function of the Volumetric Flow-Rate Ratio and the Froude Number for the Nitrogen-Mercury Mixture

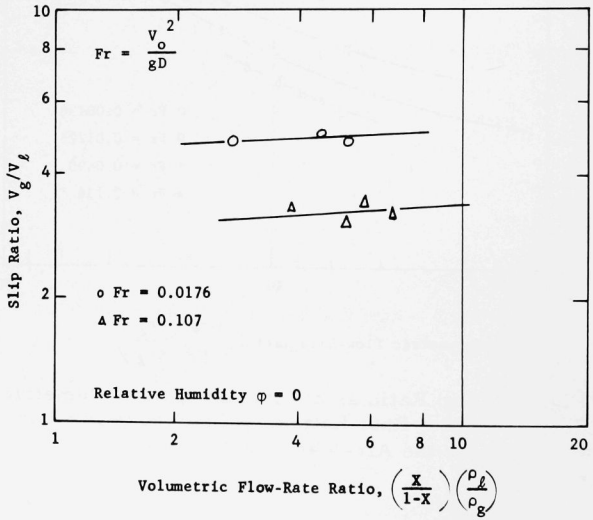

Fig. 14. Slip Ratio as a Function of the Volumetric Flow-Rate Ratio and the Froude Number for the Nitrogen-Freon-113 Mixture

Attention should be paid to the fact that slip ratios are higher in a nitrogen-mercury mixture than in an air-water mixture. Similarly, the air-water slip ratios are higher than those in the nitrogen-Freon mixture. It should be noted that the influence of the liquid density and the gas density have been eliminated by plotting the slip ratios versus the ratio of the volumetric flow rates. The fact that the curves for the various fluids were different despite the elimination of density effects leads to the conclusion that fluid properties, other than the densities, do have an influence on slippage.

The relative velocity between the gas phase and the liquid phase is presented as a function of quality and circulation rate in Figure 15 for the air-water mixture and in Figure 16 for the nitrogen-mercury mixture. The relative velocity is seen to increase with both the quality and the superficial liquid velocity. The variation of the relative velocity as a function of quality is linear except in the low-quality range in which bubble flow occurs. This clearly illustrates that the bubble-flow pattern is governed by physical laws which are different from those that are pertinent to the slug- or churn-flow patterns. It should be noted that all lines converge toward the value of the terminal velocity of a single bubble rising in a fluid.

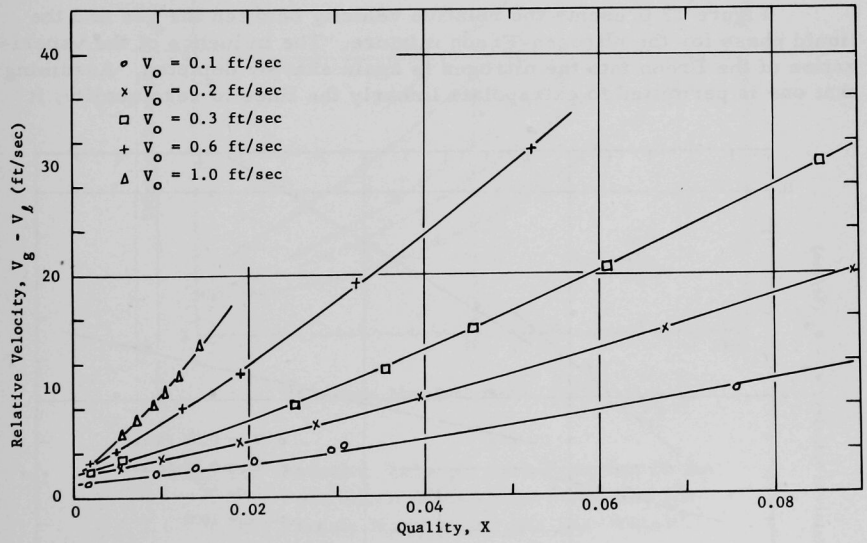

Fig. 15. Relative Velocity as a Function of Quality and Superficial Liquid Velocity for the Air-Water Mixture

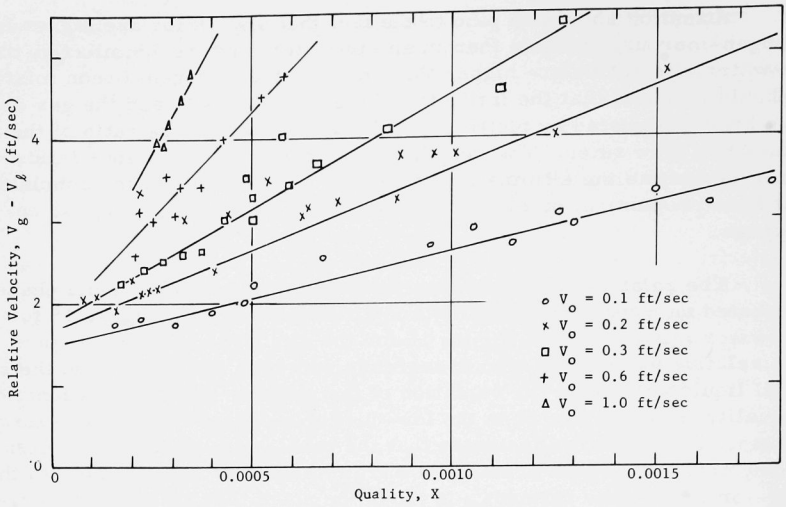

Fig. 16. Relative Velocity as a Function of Quality and Superficial Liquid Velocity for the Nitrogen-Mercury Mixture

Figure 17 presents the relative velocity between the gas and the liquid phase for the nitrogen-Freon mixture. The influence of the vaporization of the Freon into the nitrogen is again sharply depicted. Assuming that one is permitted to extrapolate linearly the lines to zero quality, it

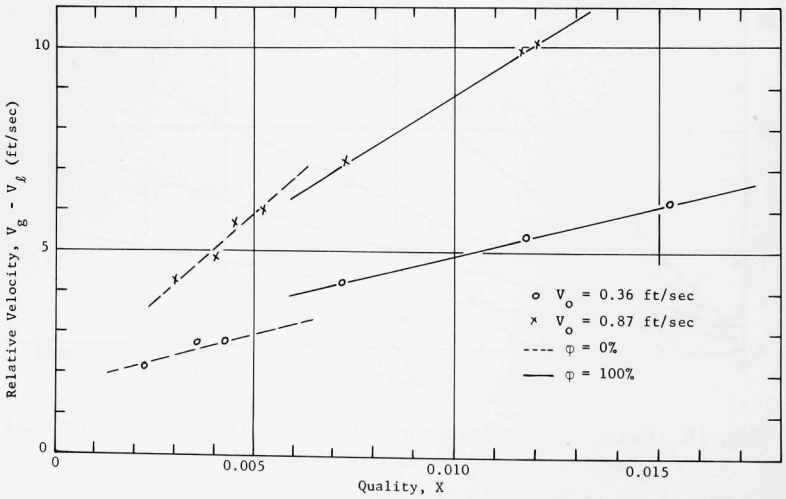

Fig. 17. Relative Velocity as a Function of Quality and Superficial Liquid Velocity for the Nitrogen-Freon-113 Mixture

becomes apparent that a gas bubble into which Freon is evaporating will have a higher terminal velocity than a gas bubble which is not subject to humidification.

The relative velocities are plotted versus the ratio of the volumetric flow rates in Figures 18, 19, and 20. Attention should be paid to the similarity between Figure 18 for the air-water mixture and Figure 19 for the nitrogen-mercury mixture. Graphs, previously presented, also showed a distinct similarity between the air-water and nitrogen-mercury data. This similarity is used in Chapter V as the basis for the hypothesis that it is possible to combine slip ratios for fluids with different properties into one general correlation.

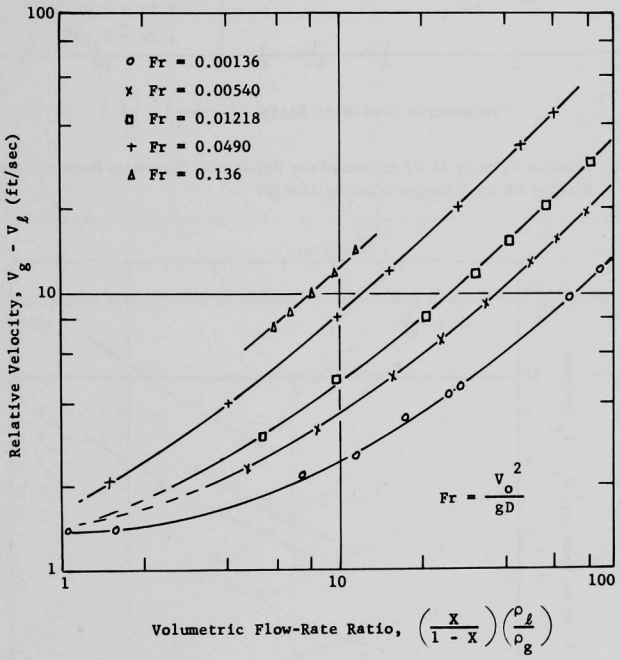

Fig. 18. Relative Velocity as a Function of the Volumetric Flow-Rate Ratio and the Froude Number for the Air-Water Mixture

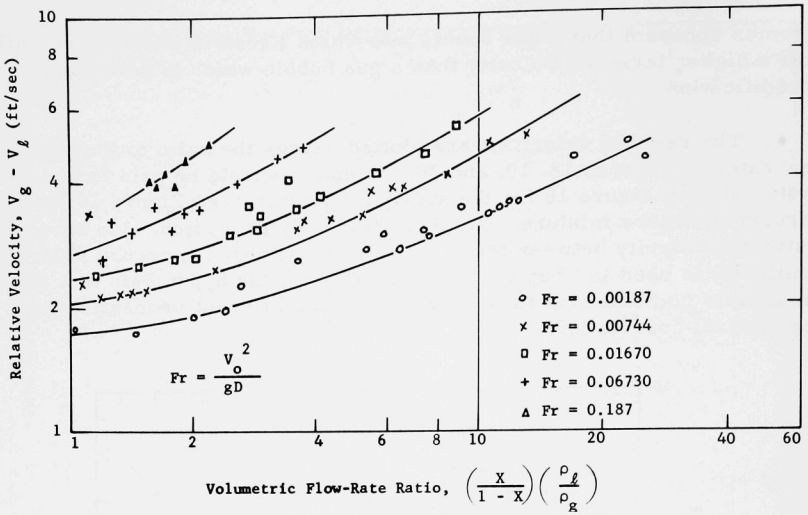

Fig. 19. Relative Velocity as a Function of the Volumetric Flow-Rate Ratio and the Froude Number for the Nitrogen-Mercury Mixture

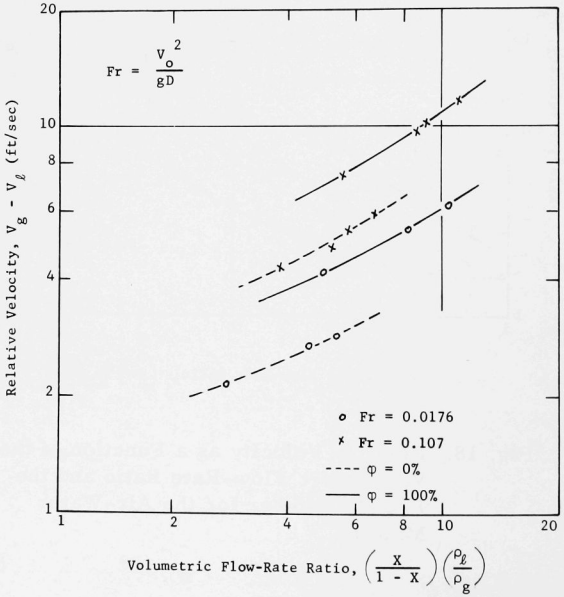

Fig. 20. Relative Velocity as a Function of the Volumetric Flow-Rate Ratio and the Froude Number for the Nitrogen-Freon-113 Mixture

The void fraction has been plotted as a function of quality and circulation rate in Figure 21 for the air-water mixture, and in Figure 22 for the nitrogen-mercury mixture. Figure 21 illustrates that the void fraction

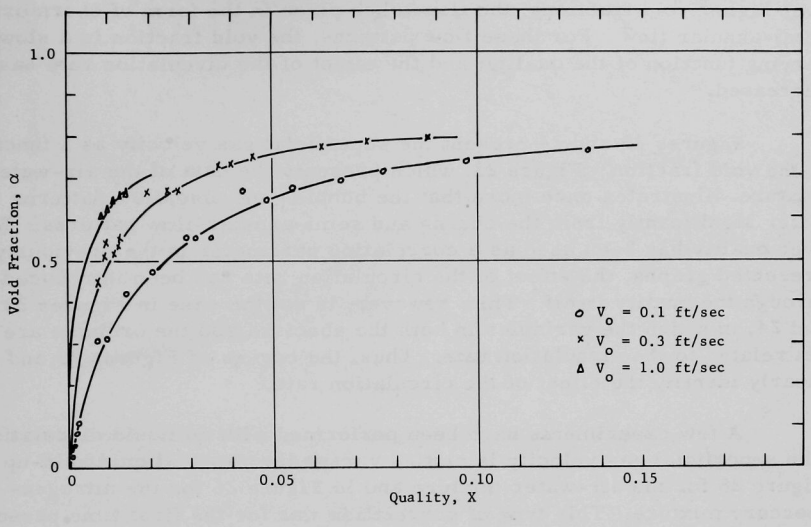

Fig. 21. Void Fraction as a Function of Quality and Superficial Liquid Velocity for the Air-Water Mixture

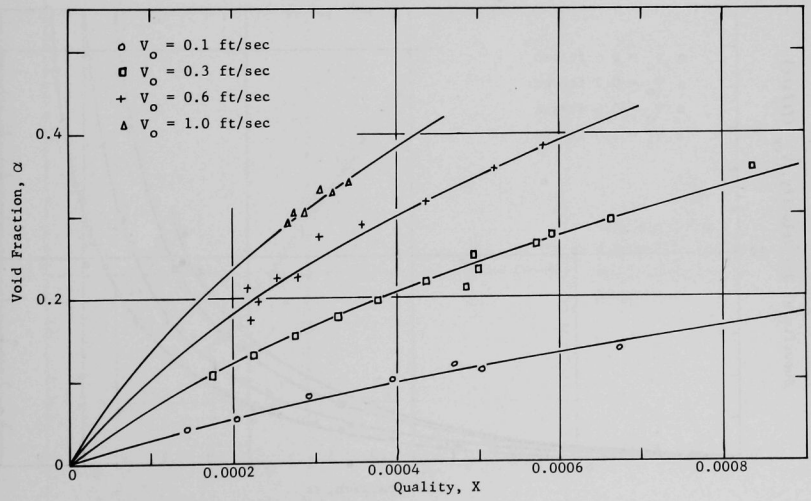

Fig. 22. Void Fraction as a Function of Quality and Superficial Liquid Velocity for the Nitrogen-Mercury Mixture

is a rapidly increasing function of the quality as long as the flow takes place in the form of bubble or slug flow. The bubble-flow pattern exists for void fractions ranging from 0 to approximately 0.280. The slug-flow pattern can be identified for void fractions between 0.280 and 0.550. For even higher void fractions, the flow takes place in the form of churn or semi-annular flow. For these flow patterns, the void fraction is a slowly varying function of the quality, and the effect of the circulation rate has decreased.

Figures 23 and 24 present the superficial gas velocity as a function of the void fraction. Figure 23, which presents the data of the air-water mixture, illustrates once more that the bubble- and slug-flow patterns differ significantly from the churn- and semi-annular-flow patterns. Whenever quality has been used as a correlating parameter in the previously presented graphs, the effect of the circulation rate has been introduced through the quality itself. This, however, is not the case in Figures 23 and 24, in which the variables in both the abscissa and the ordinate are not related to the circulation rate. Thus, the curves of Figures 23 and 24 clearly identify the effect of the circulation rate.

A few experiments have been performed with no liquid circulation. The superficial gas velocity is plotted versus the gas-to-liquid hold-up in Figure 25 for the air-water mixture and in Figure 26 for the nitrogen-mercury mixture. This type of correlation was for the first time presented by Zmola et al.[10] for air-water mixtures. Figure 25 is in good agreement with the results reported by these authors.

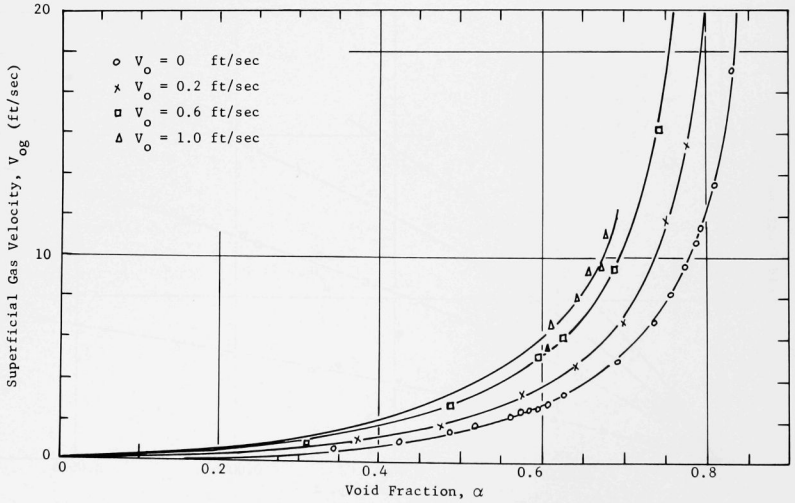

Fig. 23. Superficial Gas Velocity as a Function of Void Fraction and Superficial Liquid Velocity for the Air-Water Mixture

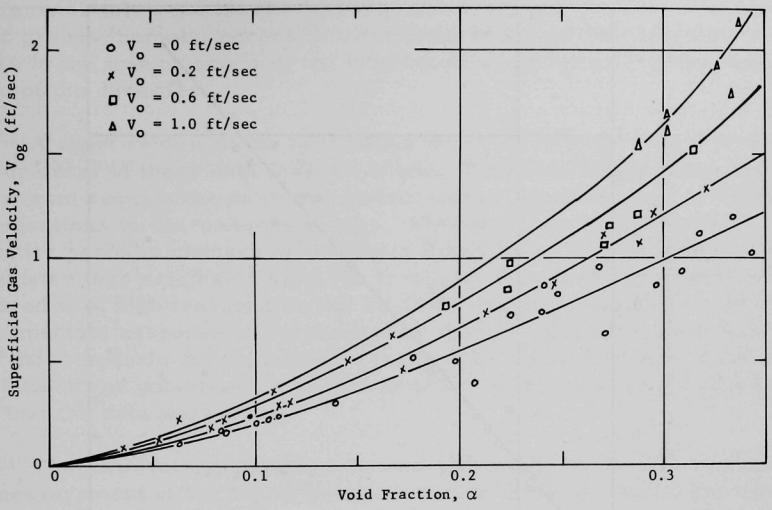

Fig. 24. Superficial Gas Velocity as a Function of Void Fraction and Superficial Liquid Velocity for the Nitrogen-Mercury Mixture

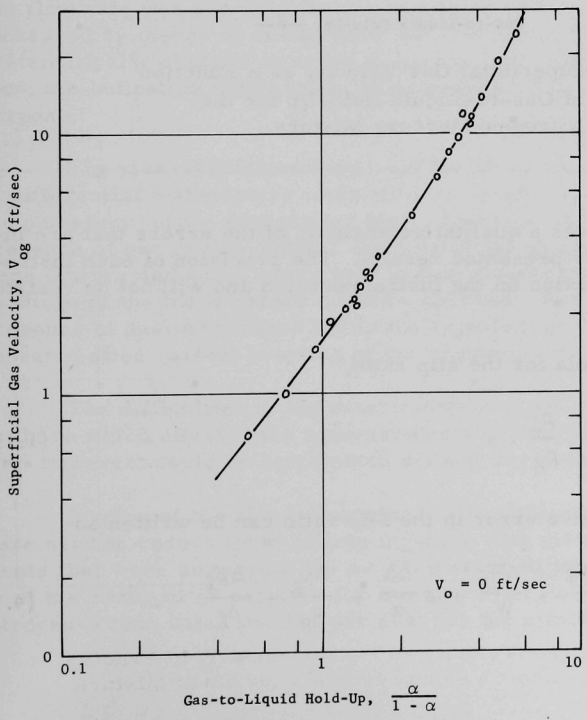

Fig. 25

Superficial Gas Velocity as a Function of Gas-to-Liquid Hold-Up for the Air-Water Mixture

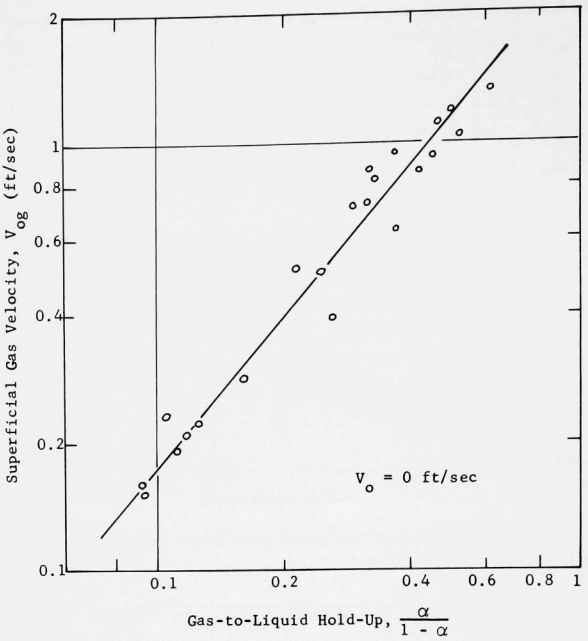

Fig. 26. Superficial Gas Velocity as a Function of Gas-to-Liquid Hold-Up for the Nitrogen-Mercury Mixture

B. Error Analysis

This section gives a qualitative analysis of the errors that are involved in the previously presented results. The precision of each instrument is given in the section on the instrumentation and will not be restated here.

From the formula for the slip ratio,

$$\frac{V_g}{V_\ell} = \frac{W_g}{W_\ell} \frac{1-\alpha}{\alpha} \frac{\rho_\ell}{\rho_g} \quad , \tag{1.15}$$

it is seen that the relative error in the slip ratio can be written as

$$\frac{\Delta(V_g/V_\ell)}{V_g/V_\ell} = \frac{\Delta W_\ell}{W_\ell} + \frac{\Delta W_g}{W_g} + 2\frac{\Delta\alpha}{\alpha} + \frac{\Delta\rho_g}{\rho_g} + \frac{\Delta\rho_\ell}{\rho_\ell} \quad . \tag{4.1}$$

It is immediately seen that the errors can be brought together into three major groups, namely, errors in the measurement of the mass flow rates, errors in the measurement of the void fraction, and errors in the determination of the densities.

A short review of the difficulties which were encountered in the measurement of these data is given below. These difficulties included transients from readjustments of the control valves, liquid-flow-rate oscillations, and pulsations in the manometer legs. Flow-rate oscillations were low-frequency periodic changes of the liquid flow rate. The pulsations in the manometer legs originated from the irregular flow in the test section. They occurred with high frequencies and could be damped out without reducing the immediate response of the measuring device. Readings were taken only after the transients from previous readjustments had died out. Flow-rate oscillations and pulsations in the manometers were visually averaged at the time that the data were taken.

The flow-rate oscillations and the pulsations in the manometers made the measurement of the liquid flow rate rather difficult. Sufficient time was spent to ascertain that the averaged value of the manometer reading corresponded to the desired flow rate. The measurement of the gas flow rate, however, was not influenced by the difficulties described above because the gas flow rate was supplied from a regulated source. Both flow rates were measured by means of orifice flow meters, the orifice plates of which were systematically changed in order to operate with the highest possible precision; the indicating fluids in the manometers were changed for the same purpose.

The measurements of the void fractions which were done by means of differential manometers were affected by both the flow oscillations and the pulsations in the manometer legs. Extreme care was taken to avoid the presence of gas in the vertical sections of the manometer lines. The runs were interrupted about every four to five measurements so that the zero readings of the manometers could be checked. Any indication of the possible presence of gas in the lines led to the rejection of the data, and the run was repeated after careful bleeding of the manometer lines.

The difficulties in the determination of the gas density were the same as those which affected the measurements of void fraction. The liquid density, however, could be determined without any appreciable error.

In view of the above-described difficulties, and the techniques that were used to reduce their effects together with the precision of the instruments that were employed, the average error of the slip ratios is thought to be of the order of ±7 per cent for the air-water data, ±15 per cent for the nitrogen-Freon data, and ±11 per cent for the nitrogen-mercury data.

V. DEVELOPMENT OF A GENERAL CORRELATION

The results presented in Chapter IV clearly illustrated the influence of both the quality and the circulation rate on slippage. The plotting of the slip ratios versus the ratio of the volumetric flow rates eliminated the effect of the densities. A comparison between the data for the three mixtures indicated that slippage is influenced not only by the density of the fluids but also by the other fluid properties. In this chapter, an attempt will be made to identify these fluid properties and to determine the importance of their effect.

The procedure used for this purpose is based on the hypothesis that it is possible to combine the slip ratios of the three mixtures into one general correlation. Dimensional analysis was used to determine suitable dimensionless groups. The resulting correlation was found to fit the data well. It was possible to derive an empirical relation to predict slip ratios as a function of flow parameters and fluid properties. Slip-quality curves which were constructed by means of this relation, however, showed slopes which were slightly different from the slopes of the curves presented in Figures 8, 9, 10, and 11. The following correlation is, therefore, not a substitute for the slip-quality graphs which were presented in Chapter IV. The correlation is valuable, however, in that it gives insight into the relative importance of the independent variables which influence slippage.

A. Dimensional Analysis

The independent variables which were believed to affect slippage in upward cocurrent flow were the gas flow rate W_g, the liquid flow rate W_ℓ, the gas density at the test point, ρ_g, the liquid density at the test point, ρ_ℓ, the dynamic viscosity of the liquid, μ_ℓ, the surface tension of the liquid, σ, the diameter of the test section, D, and the acceleration due to gravity, g. Any product of V_g and V_ℓ together with the above-listed variables has the following form,

$$\pi = (W_g)^{k_1} (W_\ell)^{k_2} (\rho_g)^{k_3} (\rho_\ell)^{k_4} (\mu_\ell)^{k_5} (\sigma)^{k_6} (D)^{k_7} (g)^{k_8} (V_g)^{k_9} (V_\ell)^{k_{10}} \qquad (5.1)$$

If the appropriate dimensions are inserted, there is obtained

$$\pi = \left(\frac{M}{T}\right)^{k_1} \left(\frac{M}{T}\right)^{k_2} \left(\frac{M}{L^3}\right)^{k_3} \left(\frac{M}{L^3}\right)^{k_4} \left(\frac{M}{LT}\right)^{k_5} \left(\frac{M}{T^2}\right)^{k_6} \left(L\right)^{k_7} \left(\frac{L}{T^2}\right)^{k_8} \left(\frac{L}{T}\right)^{k_9} \left(\frac{L}{T}\right)^{k_{10}} . \qquad (5.2)$$

The condition that the exponent of every dimension is zero gives three equations with nine unknowns:

$$k_1 + k_2 + k_3 + k_4 + k_5 + k_6 = 0 \quad , \qquad (5.3)$$

$$-k_1 - k_2 - k_5 - 2k_6 - 2k_8 + k_{10} = 0 \quad , \qquad (5.4)$$

$$-3k_3 - 3k_4 - k_5 + k_7 + k_8 - k_9 - k_{10} = 0 \quad . \qquad (5.5)$$

Equations (5.3), (5.4), and (5.5) can be rearranged and k_2, k_4, and k_7 expressed in terms of the other exponents:

$$k_2 = -k_1 - k_5 - 2k_6 - 2k_8 + k_9 + k_{10} \quad , \tag{5.6}$$

$$k_4 = -k_3 + k_6 + 2k_8 - k_9 - k_{10} \quad , \tag{5.7}$$

$$k_7 = k_5 + 3k_6 + 5k_8 - 2k_9 - 2k_{10} \quad . \tag{5.8}$$

Substitution of these variables into Equation (5.1) and grouping the terms according to common exponent give

$$\frac{V_g}{V_\ell} = f\left[\left(\frac{W_g}{W_\ell}\right)\left(\frac{\rho_\ell}{\rho_g}\right)\left(\frac{\sigma}{\mu_\ell V_0}\right)\left(\frac{V_0^2}{gD}\right)\right] \quad . \tag{5.9}$$

The group $W_g/W_\ell = X/(1-X)$ is the ratio of the gas flow rate to the liquid flow rate. The group ρ_ℓ/ρ_g is the ratio of the liquid density to the gas density and includes the effect of the pressure in the term ρ_g. The significance of the group $\sigma/\mu_\ell V_0$ becomes apparent when multiplying the numerator and the denominator by D; it is the ratio of the surface tension forces to the viscous shear forces. The surface tension forces originate from the interaction between the liquid phase and the gas phase at the gas-liquid interface. The viscous shear forces find their origin in the velocity distribution existing in the liquid phase. The last group, V_0^2/gD, is readily recognized as the Froude number and is the ratio of the inertial to the gravitational or weight forces. The significance of this group becomes apparent when multiplying and dividing by $\rho_\ell A_p$. It is left to determine the functional relation between the slip ratio and the dimensionless groups of Equation (5.9).

B. Derivation of a General Correlation

A cross-plot of the graphs presented in Figures 12, 13, and 14 revealed that the lines of constant Froude number could be brought together by multiplying the slip ratios by the dimensionless group $(\sigma/\mu_\ell V_0)$ raised to a power of 0.300. A family of curves with the Froude number as parameter was obtained. This family of curves could be combined when the Froude number was raised to a variable exponent which was a linear function of the logarithm of the volumetric flow rate ratio. A first attempt to correlate the slip ratios of the three mixtures revealed a functional relation of the form

$$\ell n\left(\frac{V_g}{V_\ell}\right) = \ell n\, C_1 + \ell n\left[\left(\frac{X}{1-X}\right)\left(\frac{\rho_\ell}{\rho_g}\right)\left(\frac{\sigma}{\mu_\ell V_0}\right)^{C_2}\left(\frac{V_0^2}{gD}\right)^{C_3}\right] \quad , \tag{5.10}$$

where

$$C_3 = C_4 - C_5 \log_{10}\left[\left(\frac{X}{1-X}\right)\left(\frac{\rho_\ell}{\rho_g}\right)\right] \quad . \tag{5-11}$$

The best combination of the constants C_1, C_2, C_4, and C_5 was determined by a statistical analysis. A selection was made of 124 data points (out of a total of 294) in such a way that for each mixture and for each circulation rate both the maximum and the minimum deviations from the expected value would be included. A digital computer program was developed to perform this work. The program computed the least-square best fit for the data for various combinations of C_1, C_2, C_4, and C_5. It also permitted computation of the deviation (in per cent) of each point from the line of best fit. The procedure for determining the best combination of constants consisted in minimizing the standard deviation of the per cent deviations of all points. The correlation which was found to be the "best" for the data set is written as

$$\frac{V_g}{V_\ell} = 0.815 \left[\left(\frac{X}{1-X} \right) \left(\frac{\rho_\ell}{\rho_g} \right) \left(\frac{\sigma}{\mu_\ell V_0} \right)^{0.700} \left(\frac{V_0^2}{gD} \right)^{-A} \right]^{0.416} , \qquad (5.12)$$

with

$$A = 0.420 - 0.135 \log_{10} \left[\left(\frac{X}{1-X} \right) \left(\frac{\rho_\ell}{\rho_g} \right) \right] . \qquad (5.13)$$

The correlation of Equations (5.12) and (5.13) is displayed in Figure 27.

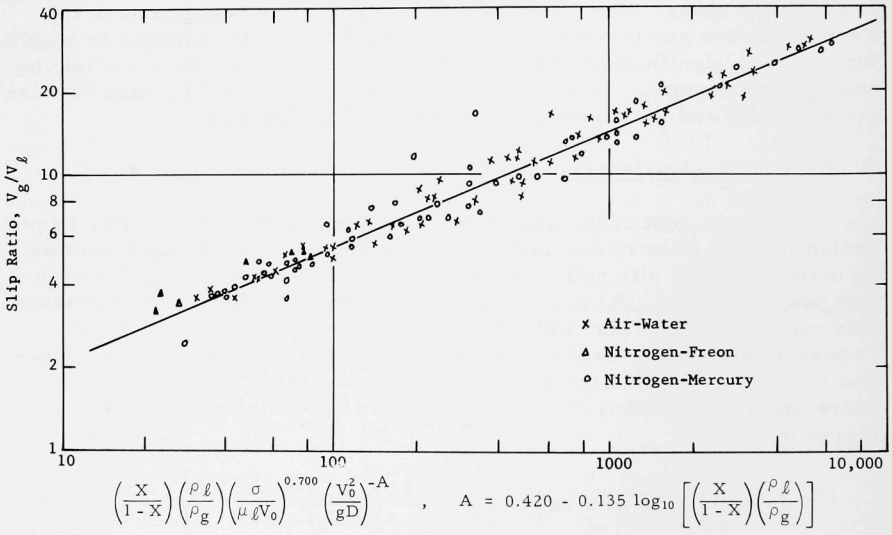

Fig. 27. Dimensionless Correlation for Slip Ratios

A close fit exists over the entire range of slip ratios. The distribution of the per cent error of the data is given in Figure 28. This distribution has a standard deviation of

$$\sigma = 0.137 \quad . \tag{5.14}$$

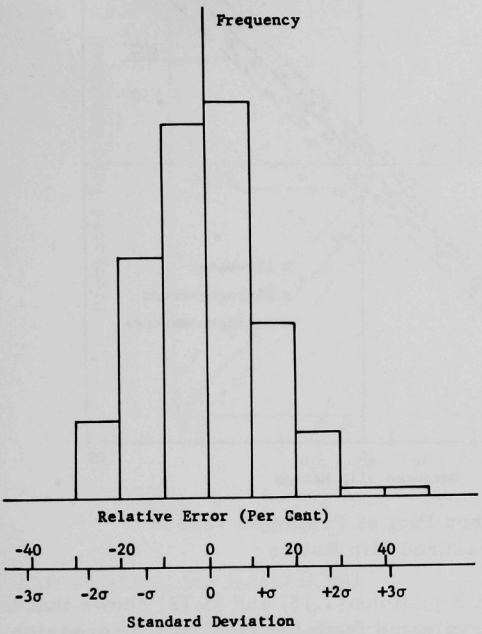

Fig. 28

Error Distribution of Slip-Ratio Correlation

Equation (5.12) can also be written as

$$\frac{V_g}{V_\ell} = 0.815 \left[\left(\frac{X}{1-X}\right)\left(\frac{\rho_\ell}{\rho_g}\right)\right]^{0.416} \left(\frac{\sigma}{\mu_\ell V_0}\right)^{0.29} \left(\frac{V_0^2}{gD}\right)^{-B} \quad , \tag{5.15}$$

where

$$B = 0.416\, A = 0.175 - 0.056 \log_{10}\left[\left(\frac{X}{1-X}\right)\left(\frac{\rho_\ell}{\rho_g}\right)\right] \quad . \tag{5.16}$$

Equations (5.15) and (5.16) can be used to evaluate the slip ratio as a function of the flow parameters and the fluid properties for superficial liquid velocities ranging from 0 to 1 ft/sec, and pipe diameters larger than 2 in. Figure 29 gives an error plot of the measured values of the slip ratios versus the values predicted by Equations (5.15) and (5.16).

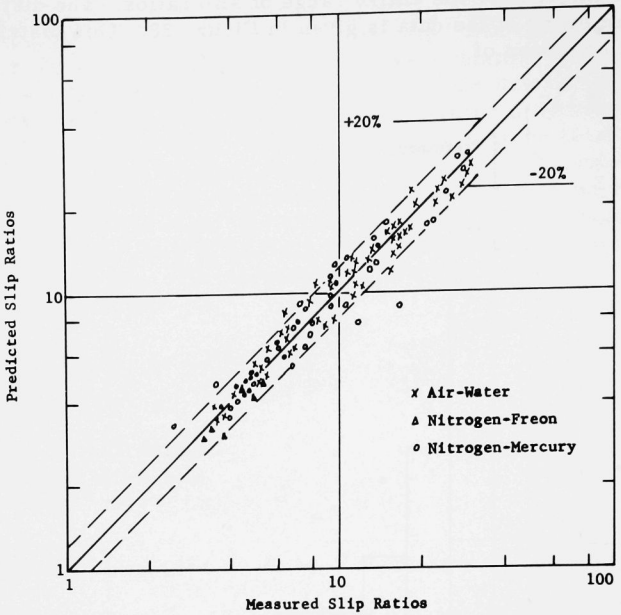

Fig. 29. Error Plot of Predicted versus Measured Slip Ratios

A comparison between Equations (1.15) and (5.12) shows that the liquid-to-gas hold-up can be evaluated from the empirical expression

$$\frac{1-\alpha}{\alpha} = 0.815\left[\left(\frac{X}{1-X}\right)\left(\frac{\rho_\ell}{\rho_g}\right)\right]^{-0.584}\left(\frac{\sigma}{\mu_\ell V_0}\right)^{0.29}\left(\frac{V_0^2}{gD}\right)^{-B} , \qquad (5.17)$$

with

$$B = 0.175 - 0.056 \log_{10}\left[\left(\frac{X}{1-X}\right)\left(\frac{\rho_\ell}{\rho_g}\right)\right] . \qquad (5.16)$$

An error plot of the measured void fractions versus those predicted by Equations (5.17) and (5.16) is given in Figure 30.

The empirical relations which were presented for the prediction of slip ratios and void fractions are valid in the parameter ranges specified in Table I. They are recommended for flow regimes with void fractions ranging from 0.100 to 0.800 and apply to volumetric flow rate ratios ranging from 0.600 to 100. Care should be used in extrapolating the correlation outside the ranges specified above.

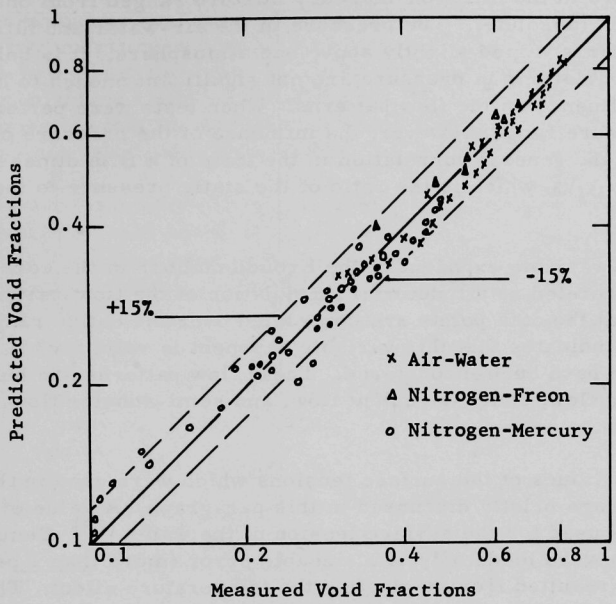

Fig. 30. Error Plot of Predicted versus Measured Void Fractions

C. Discussion of the Correlation

Seven independent variables are included in the general correlation, namely, the quality, the superficial liquid velocity, the liquid density, the gas density, the surface tension of the liquid, the viscosity of the liquid, and the pipe diameter. The gas density, however, includes the effects of temperature and pressure. The effect of the temperature is also introduced through the liquid properties, i.e., through the surface tension, the viscosity, and the density.

The effects of the gas viscosity and the pressure were not included in the dimensional analysis. Whether or not the viscosity of the gas phase has an influence on slippage is not known. One would expect that the gas viscosity does have an influence, but its importance has not been investigated yet. The two gases that were used in the experiments, air and nitrogen, have practically the same viscosity. Any influence of this fluid property was therefore eliminated. The pressure has not been included in the dimensional analysis, unless indirectly through the gas density. It has been explained in the "Introduction" that the pressure has a dual influence on slippage, namely, changing the gas density and affecting the flow patterns. The pressure range which was covered in the experiments was rather small.

The pressure in the nitrogen-mercury mixture ranged from one to two atmospheres (absolute). The pressure in the air-water and nitrogen-Freon mixtures varied slightly above one atmosphere. It is believed that these variations in pressure are not significant enough to have a sizeable influence on the flow patterns. When tests were performed in a wider pressure range, however, the influence of the pressure could be included in the general correlation in the form of a fifth dimensionless group, $g_c P/\rho_\ell V_0^2$, which is the ratio of the static pressure to the dynamic pressure.

The variable exponent of the Froude number in the correlation can be interpreted as a functional formulation of the flow-pattern effect. The fact that the data points are correlated over the entire range of the slip ratios indicates that this variable exponent is valid for all flow patterns which have been encountered. These flow patterns are bubble flow, slug or plug flow, churn-turbulent flow, and semi-annular flow, respectively.

The values of the surface tensions which were used in the general correlation are briefly discussed in this paragraph. A value of 0.005 lb_f/ft at 66°F was used for the surface tension of the water.[35] Temperature corrections were made only if a sizeable error (more than 1 per cent) would have resulted from neglecting the temperature effect. The values of the surface tension of mercury which are reported in the literature[35-38] vary over a range of 6 per cent. An average value of 0.03 lb_f/ft was used in the correlation. The surface tension of the Freon was 0.0013 lb_f/ft.[39]

Equations (5.15) and (5.16) were used to reconstruct the slip-quality graphs of Figures 8, 9, 10, and 11. It was observed that the slopes of the reconstructed curves were slightly different from those of the best-fit lines. The air-water reconstructed curves had a lower slope than the measured curves; the nitrogen-mercury lines, however, showed the opposite trend. This indicates that some effects or independent variables were omitted in the derivation of the general correlation. An attempt was made to include the dimensionless group $g_c P/\rho_\ell V_0^2$ into the correlation, but this did not bring any improvement.

The cause of the above-mentioned discrepancy between the slopes could not be determined. The development of the general correlation was based on the hypothesis that slip ratios for fluids with different properties can be brought together into one correlation. There is no evidence to date that this hypothesis is valid. Neal[18] concluded in a recent study of cocurrent nitrogen-mercury flow that the correlations developed for air-water mixtures were not valid for nitrogen-mercury mixtures. This conclusion was based on results which were obtained from experiments in a non-wetted test section. The type of flow which was observed in that case

was entirely different from the types generally identified in wetted pipes. The nitrogen-mercury experiments of the present study, however, were carried out in a mercury-wetted test section. Whether the wetting of the wall by mercury gives flow types which are completely similar to those in air-water mixtures could not be observed and has yet to be confirmed. Thus, it is possible that the assumption of similar flow types in the three mixtures was not valid; this would explain the difference in slopes.

A second reason for the discrepancy in the slip-quality slopes could be found in an inadequate or incomplete choice of independent variables with which the dimensional analysis was performed. It is believed that more two-phase mixtures should be tested to determine the validity of this assumption.

VI. SUMMARY AND CONCLUSIONS

This study was undertaken with the purpose of providing slip-ratio data for gas-liquid mixtures which circulate with superficial liquid velocities ranging from 0 to 1 ft/sec. The need for these data originated from the fact that existing correlations failed to predict accurately slip ratios when the mixture was moving at a slow rate. The experimental study involved the determination of slip ratios, relative velocities, void fractions, and superficial gas velocities as a function of quality and circulation rate in air-water, nitrogen-Freon-113, and nitrogen-mercury mixtures. All experiments were carried out in natural-circulation loops under atmospheric pressure, and the test sections were chosen large enough to avoid geometry effects. The nitrogen-mercury mixture was studied in a mercury-wetted test section. This avoided the formation of large gas slugs and the subsequent unstable flow pattern which is characterized by severe static pressure oscillations. A comparison was made between the slip ratios obtained in each of the three mixtures with the purpose of identifying the influence of fluid properties on gas slippage.

It was observed that two-phase flow parameters were strongly dependent upon both the quality and the superficial liquid velocity. Slip ratios and relative velocities were plotted versus the ratio of the volumetric flow rates. A family of curves was obtained with the Froude number, which was based on the superficial liquid velocity, as a parameter. The graph for the air-water slip ratios was observed to deviate significantly from the working graph which was proposed by Marchaterre and Hoglund[6] for superficial liquid velocities higher than 0.8 ft/sec.

It was found that fluid properties have significant influences on slippage in gas-liquid mixtures. Slip ratios were observed to increase with increasing surface tension, and to decrease with increasing dynamic viscosity of the liquid. The effect of flow patterns was found to be conveniently described by a variable exponent of the Froude number. This exponent could be expressed as a linearly decreasing function of the logarithm of the volumetric flow rate ratio. Dimensional analysis was used to derive empirical relations for the prediction of slip ratios and void fractions as a function of the flow parameters and the fluid properties:

$$\frac{V_g}{V_\ell} = 0.815 \left[\left(\frac{X}{1-X}\right)\left(\frac{\rho_\ell}{\rho_g}\right)\right]^{0.416} \left(\frac{\sigma}{\mu_\ell V_0}\right)^{0.29} \left(\frac{V_0^2}{gD}\right)^{-B} \quad ; \qquad (5.15)$$

$$\frac{1-\alpha}{\alpha} = 0.815 \left[\left(\frac{X}{1-X}\right)\left(\frac{\rho_\ell}{\rho_g}\right)\right]^{-0.584} \left(\frac{\sigma}{\mu_\ell V_0}\right)^{0.29} \left(\frac{V_0^2}{gD}\right)^{-B} \quad , \qquad (5.17)$$

with

$$B = 0.175 - 0.056 \log_{10} \left[\left(\frac{X}{1-X} \right) \left(\frac{\rho_\ell}{\rho_g} \right) \right] \quad . \tag{5.16}$$

These empirical relations were determined for two-phase mixtures which were flowing at superficial liquid velocities ranging from 0 to 1 ft/sec, with corresponding void fractions ranging from 0.100 to 0.800. They are not recommended for the prediction of slip ratios in pipes with inner diameters less than 2 in. The empirical relations predicted 95 per cent of the slip ratio data with a maximum relative error of ±27.2 per cent, and 95 per cent of the void fraction data with a maximum relative error of ±15 per cent.

This study provides foundations upon which other studies can be carried out. The fluids which were used in this experimental study had surface tensions whose values varied over a wide range. As a result, the effect of the surface tension could easily be observed. The values of the dynamic viscosities of the liquid, however, were restricted to a narrow range, and the presence of μ_ℓ in the denominator of the dimensionless group $\sigma/\mu_\ell V_0$ was justified on the basis of dimensional analysis. It is suggested that tests be made to experimentally confirm the validity of this group as a correlating parameter.

The influence of the viscosity of the gas was not investigated in this study. More experimental data are needed to identify the importance of this fluid property.

Dimensional analysis permitted a correlation of slip ratios and void fractions as a function of flow parameters and fluid properties in a parameter range which was restricted to low circulation rates, large pipe diameters, and atmospheric pressure. An attempt should be made to apply this correlating procedure to slip ratios and void fractions which hold for conditions outside the range of this work.

VII. BIBLIOGRAPHY

1. Moore, T. V., and H. D. Wilde, Experimental Measurement of Slippage in Flow through Vertical Pipes, Trans. AIME, Petr. Div. (1931).

2. Peebles, F. N., and H. J. Garber, Studies on the Motion of Gas Bubbles in Liquids, Chem. Eng. Progress, 49 (Feb 1953).

3. Martinelli, R. C., L. M. K. Boelter, T. H. M. Taylor, E. G. Thomson, and E. H. Morrin, Isothermal Pressure Drop for Two-phase, Two-component Flow in a Horizontal Pipe, Trans. ASME, 66 (Feb 1944).

4. Martinelli, R. C., and D. B. Nelson, Prediction of Pressure Drop during Forced Circulation Boiling of Water, Trans. ASME, 70 (Aug 1948).

5. Lockhart, R. W., and R. C. Martinelli, Proposed Correlation of Data for Isothermal Two-phase, Two-component Flow in Pipes, Chem. Eng. Progress, 45 (Jan 1949).

6. Marchaterre, J. F., and B. M. Hoglund, Correlation for Two-phase Flow, Nucleonics, 20 (Aug 1962).

7. Petrick, M., Two-phase Air-Water Flow Phenomena, ANL-5787 (March 1958).

8. Marchaterre, J. F., and M. Petrick, The Prediction of Steam Volume Fractions in Boiling Systems, Nuclear Science and Engineering, 7 (June 1960).

9. Kutateladze, S. S., Heat Transfer in Condensation and Boiling, AEC-tr-3770 (Aug 1959).

10. Zmola, P. C., R. V. Bailey, F. M. Taylor, and R. J. Planchet, Transport of Gases through Liquid-Gas Mixtures, ORNL-55-12-18, Presented at the Symposium on Fundamental Mechanisms in Boiling, Cavitation and Condensation, AIChE, New Orleans, May 6-9, 1956.

11. Marchaterre, J. F., M. Petrick, P. A. Lottes, R. J. Weatherhead, and W. S. Flinn, Natural and Forced Circulation Boiling Studies, ANL-5735 (May 1960).

12. Marchaterre, J. F., The Effect of Pressure on Boiling Density in Multiple Rectangular Channels, ANL-5522 (Feb 1956).

13. Petrick, M., A Study of Vapor Carryunder and Associated Problems, ANL-6581 (July 1962).

14. Levy, S., Steam Slip-Theoretical Prediction from Momentum Model, Journ. of Heat Transfer, Trans. ASME Series C, 82 (May 1960).

15. Siemes, Gas Bubbles in Fluids, Part I: Chemie Ing.-Techn., 26 Jahrg. No. 8/9 (Aug-Sept 1954); Part II: Chemie Ing.-Techn., 26 Jahrg. No. 11 (Nov 1954).

16. Zuber, N., and J. Hench, Steady State and Transient Void Fraction of Bubbling Systems and their Operating Limits, Part I: Steady State Operation, G. E. Report No. 62GL100 (July 1962).

17. Isbin, H. S., N. C. Sher, and K. C. Eddy, Void Fractions in Two-phase Steam-Water Flow, AIChE Journ., 3 (March 1957).

18. Neal, L. G., Local Parameters in Cocurrent Mercury-Nitrogen Flow, ANL-6625 (Jan 1963).

19. Schwarz, K., Investigation of the Distribution of the Density, Water and Steam Velocity, and of the Pressure Loss in Vertical and Horizontal Up-flow Boiler Tubes, V. D. I. Forschungsheft, 445B (1954).

20. Behringer, P., Velocity of the Rise of Steam Bubbles in Boiler Tubes, V. D. I. Forschungsheft, 365B (1934).

21. Schurig, W., Water Circulation in Boilers and Movement of Liquid-Gas Mixtures in Tubes, V. D. I. Forschungsheft, 365B (1934).

22. Lottes, P. A., and W. S. Flinn, A Method of Analysis of Natural Circulation Boiling Systems, Nuclear Science and Engineering, 1 (Dec 1956).

23. Cook, W. H., Boiling Density in Vertical Rectangular Multi-channel Sections with Natural Circulation, ANL-5621 (Nov 1956).

24. Egen, R. A., D. A. Dingee, and J. W. Chastain, Vapor Formation and Behavior in Boiling Heat Transfer, BMI-1163 (Feb 1957).

25. Dengler, C. E., Heat Transfer and Pressure Drop for Evaporation of Water in Vertical Tubes, Unpublished Sc.D. Thesis, Massachusetts Institute of Technology (1952).

26. Eddy, K. D., Pressure Ratios in Two-phase Flow, Unpublished M.S. Thesis, University of Minnesota (1954).

27. Sher, N. C., Liquid Hold-up in Two-phase Steam-Water Flow, Unpublished Thesis, University of Minnesota (1954).

28. Galegar, W. C., W. B. Stoval, and R. L. Huntington, More Data on Two-phase Vertical Flow, Petroleum Refiner, 33 (Nov 1954).

29. Liquid Metals Handbook, Sodium-Nak Supplement, p. 51.

30. Bonilla, C., and Misza, Heat Transfer in the Condensation of Metal Vapors: Mercury and Sodium up to Atmospheric Pressure, Heat Transfer, Chem. Eng. Progress, Symposium Series, 52 (1956).

31. Hacket, H. N., Mercury for the Generation of Light, Heat and Power, Trans. ASME, 64 (Oct 1942).

32. Hooker, H. H., and G. F. Popper, A Gamma-ray Attenuation Method for Void Fraction Determination in Experimental Boiling Heat Transfer Test Facilities, ANL-5766 (Nov 1958).

33. Grace, H. P., and G. E. Lapple, Discharge Coefficients of Small-diameter Orifices and Flow Nozzles, Trans. ASME, 73 (July 1951).

34. Thermodynamic Properties of "Freon-113" Trichlorotrifluoroethane, with Addition of Other Physical Properties, E. I. Du Pont de Nemours & Company, "Freon" Products Division, Wilmington 98, Delaware.

35. Streeter, V. L., Fluid Mechanics, McGraw-Hill Book Company, Inc., New York (1962) Third Edition, p. 14.

36. Handbook of Chemistry and Physics, Chemical Rubber Publishing Company (1961-1962) Forty-Fourth Edition, p. 2197.

37. Streeter, V. L., Handbook of Fluid Dynamics, McGraw-Hill Book Company, Inc., New York (1961) First Edition, p. 1-19.

38. Metals Handbook, American Society for Metals (1961) Vol. I, Eighth Edition, p. 1215.

39. Surface Tension of the Freon Compounds, E. I. Du Pont de Nemours & Company, "Freon" Products Division, Wilmington 98, Delaware.

APPENDIX

I. TABULATED DATA FOR AIR-WATER MIXTURE

Run Number	V_o (ft/sec)	X	α	$\frac{V_g}{V_\ell}$	$V_g - V_\ell$ (ft/sec)	V_{og} (ft/sec)	$\left(\frac{X}{1-X}\right)\left(\frac{\rho_\ell}{\rho_g}\right)$
A-1	0	-	0.597	-	-	2.87	-
2	↓	-	0.600	-	-	2.74	-
3		-	0.584	-	-	2.53	-
4		-	0.553	-	-	2.31	-
5		-	0.553	-	-	2.09	-
6		-	0.514	-	-	1.84	-
7		-	0.481	-	-	1.41	-
8		-	0.419	-	-	0.97	-
9		-	0.339	-	-	0.69	-
10		-	0.778	-	-	11.80	-
11		-	0.784	-	-	11.30	-
12		-	0.783	-	-	10.60	-
13		-	0.766	-	-	9.45	-
14		-	0.752	-	-	8.19	-
15		-	0.733	-	-	6.65	-
16		-	0.689	-	-	4.68	-
17		-	0.619	-	-	3.32	-
18		-	0.577	-	-	2.63	-
19		-	0.847	-	-	23.78	-
20		-	0.823	-	-	18.90	-
21		-	0.803	-	-	13.29	-
B-1	0.10	0.0763	0.703	28.60	9.28	6.78	67.80
2	↓	0.0661	0.691	25.90	-	-	57.88
3		0.0545	0.666	23.40	-	-	46.60
4		0.0492	0.644	23.30	-	-	42.16
5		0.0313	0.559	20.60	4.43	2.61	26.10
6		0.1260	0.763	37.20	15.20	12.02	119.46
7		0.0964	0.744	28.60	11.50	8.80	88.17
8		0.0428	0.666	18.30	-	-	36.45
9		0.0349	0.559	23.30	-	-	29.48
10		0.0293	0.566	18.80	4.11	2.45	24.56
11		0.0205	0.475	18.70	3.54	1.69	16.87
12		0.0137	0.419	15.50	2.48	1.12	11.16
13		0.0089	0.303	16.40	2.22	0.711	7.15
14		0.0020	0.108	12.10	1.34	0.156	1.56
15		0.0018	0.092	13.90	-	-	1.41
16		0.0013	0.067	14.20	1.42	0.105	1.02
17		0.2200	0.828	49.30	-	-	236.50
18		0.1880	0.803	47.50	-	-	193.95
19		0.1550	0.788	41.10	-	-	153.01
20		0.1133	0.780	29.82	-	-	105.74
21		0.0932	0.753	27.95	-	-	85.21
22	↓	0.0775	0.738	25.40	-	-	69.04

Run Number	V_0 (ft/sec)	X	α	$\frac{V_g}{V_\ell}$	$V_g - V_\ell$ (ft/sec)	V_{0g} (ft/sec)	$\left(\frac{X}{1-X}\right)\left(\frac{\rho_\ell}{\rho_g}\right)$
C-1	0.20	0.0390	0.694	14.70	8.95	6.79	33.40
2		0.0277	0.644	12.90	6.64	4.65	23.30
3		0.0187	0.578	11.30	4.89	3.10	15.50
4		0.0672	0.753	19.60	15.01	11.93	59.60
5		0.0528	0.728	17.20	-	-	46.10
6		0.0374	0.675	15.40	-	-	32.00
7		0.0218	0.539	15.40	-	-	18.10
8		0.0126	0.513	9.80	-	-	10.40
9		0.0103	0.475	9.30	3.15	1.67	8.39
10		0.0059	0.377	7.80	2.18	0.94	4.71
11		0.0171	0.556	11.30	-	-	14.18
12		0.0144	0.531	10.40	-	-	11.85
13		0.0111	0.498	9.10	-	-	9.05
14		0.1270	0.809	28.80	29.10	24.38	122.00
15		0.0978	0.781	25.40	-	-	91.00
16		0.0843	0.772	22.70	18.98	15.35	76.80
D-1	0.30	0.0455	0.750	13.3	15.18	11.89	39.80
2		0.0358	0.731	11.3	11.51	9.23	30.74
3		0.0241	0.678	9.7	8.05	6.09	20.35
4		0.0116	0.541	8.1	4.84	2.85	9.52
5		0.0264	0.678	10.6	-	-	22.33
6		0.0191	0.663	8.1	-	-	16.00
7		0.0103	0.516	7.9	-	-	8.43
8		0.0115	0.550	7.7	-	-	9.40
9		0.0094	0.544	6.4	-	-	7.72
10		0.0083	0.506	6.6	-	-	6.80
11		0.0065	0.450	6.5	3.11	1.58	5.31
12		0.0866	0.794	20.6	28.96	23.80	79.39
13		0.0721	0.788	17.5	-	-	64.97
14		0.0608	0.763	16.8	20.26	16.19	53.95
E-1	0.40	0.0086	0.530	6.26	4.46	2.83	7.05
2		0.0081	0.527	6.00	-	-	6.64
3		0.0073	0.509	5.80	-	-	5.96
4		0.0064	0.486	5.50	-	-	5.21
5		0.0052	0.447	5.20	-	-	4.22
6		0.0041	0.402	4.90	-	-	3.32
7		0.0029	0.338	4.60	2.15	0.93	2.32
8		0.0345	0.730	11.00	-	-	29.76
9		0.0326	0.725	10.60	-	-	27.88
10		0.0299	0.716	10.20	-	-	25.60
11		0.0268	0.709	9.40	-	-	22.85
12		0.0227	0.683	8.90	-	-	19.19
13		0.0174	0.659	7.50	7.67	5.83	14.59
14		0.0127	0.614	6.60	5.83	4.22	10.53
15		0.0104	0.570	6.50	-	-	8.58
16		0.0968	0.813	20.70	42.13	35.99	90.13
17		0.0756	0.805	16.60	32.01	27.42	68.68
18		0.0653	0.791	15.30	-	-	58.14
19		0.0545	0.778	13.60	-	-	47.85
20		0.0397	0.758	10.90	16.36	13.65	34.13
21		0.0292	0.723	9.50	-	-	24.84
22		0.0333	0.752	9.52	-	-	28.85

Run Number	V_0 (ft/sec)	X	α	$\frac{V_g}{V_\ell}$	$V_g - V_\ell$ (ft/sec)	V_{0g} (ft/sec)	$\left(\frac{X}{1-X}\right)\left(\frac{\rho_\ell}{\rho_g}\right)$
E-23	0.40	0.0289	0.728	9.29	-	-	24.85
24	↓	0.0250	0.722	8.23	-	-	21.38
25		0.0209	0.694	7.83	-	-	17.76
26		0.0166	0.650	7.51	-	-	13.97
27		0.0101	0.547	6.93	-	-	8.37
28		0.0064	0.436	6.77	-	-	5.23
F-1	0.60	0.0057	0.505	4.60	-	-	4.65
2		0.0055	0.500	4.50	-	-	4.49
3		0.0050	0.480	4.40	3.92	2.45	4.07
4		0.0044	0.464	4.10	-	-	3.57
5		0.0038	0.434	4.00	-	-	3.07
6		0.0029	0.375	3.90	-	-	2.33
7		0.0019	0.313	3.30	2.05	0.97	1.52
8		0.0233	0.719	7.80	-	-	19.88
9		0.0224	0.697	8.30	-	-	19.02
10		0.0204	0.684	8.00	-	-	17.26
11		0.0183	0.683	7.20	11.63	9.27	15.47
12		0.0148	0.658	6.40	-	-	12.38
13		0.0120	0.617	6.20	8.11	5.97	9.94
14		0.0086	0.578	5.20	-	-	7.10
15		0.0061	0.513	4.70	-	-	4.98
16		0.0674	0.794	15.60	42.55	36.07	60.22
17		0.0604	0.783	14.80	-	-	53.56
18		0.0518	0.772	13.40	32.64	27.23	45.42
19		0.0454	0.766	12.10	-	-	39.54
20		0.0316	0.734	9.80	19.85	16.18	27.00
21		0.0455	0.775	11.50	-	-	39.78
22		0.0370	0.741	11.20	-	-	32.03
23		0.0286	0.741	8.60	-	-	24.45
24		0.0222	0.728	7.08	-	-	18.93
25		0.0193	0.709	6.72	-	-	16.39
26		0.0168	0.700	6.09	-	-	14.20
27		0.0140	0.664	5.95	-	-	11.76
28		0.0105	0.616	5.43	-	-	8.72
29		0.0066	0.527	4.85	-	-	5.40
30	↓	0.0042	0.419	4.54	-	-	3.40
G-1	0.80	0.0041	0.444	4.20	-	-	3.32
2		0.0043	0.475	3.90	-	-	3.49
3		0.0037	0.444	3.70	-	-	2.99
4		0.0034	0.425	3.70	3.79	2.22	2.74
5		0.0175	0.689	6.70	-	-	14.77
6		0.0166	0.686	6.40	-	-	14.02
7		0.0154	0.666	6.50	-	-	12.92
8		0.0137	0.659	5.80	11.57	9.21	11.48
9		0.0112	0.639	5.30	-	-	9.31
10		0.0081	0.589	4.70	7.17	5.34	6.72
11		0.0059	0.534	4.20	5.50	3.88	4.81
12		0.0044	0.483	3.80	-	-	3.56
13		0.0511	0.766	13.70	-	-	44.83
14		0.0506	0.761	13.90	-	-	44.39
15		0.0333	0.747	9.70	27.61	22.97	28.69
16	↓	0.0280	0.728	9.00	-	-	23.96

Run Number	V_0 (ft/sec)	X	α	$\frac{V_g}{V_\ell}$	$V_g - V_\ell$ (ft/sec)	V_{0g} (ft/sec)	$\left(\frac{X}{1-X}\right)\left(\frac{\rho_\ell}{\rho_g}\right)$
G-17	0.80	0.0226	0.709	7.90	18.91	15.34	19.19
18		0.0142	0.664	6.00	-	-	11.90
19		0.0165	0.697	6.12	-	-	13.95
20		0.0147	0.686	5.70	-	-	12.44
21		0.0124	0.659	5.43	-	-	10.49
22		0.0098	0.620	5.04	-	-	8.23
23		0.0076	0.581	4.58	-	-	6.35
24		0.0041	0.472	3.73	-	-	3.33
25		0.0036	0.431	3.86	-	-	2.93
H-1	1.0	0.0135	0.659	5.77	14.11	11.21	11.18
2		0.0114	0.652	5.02	11.57	9.43	9.41
3		0.0097	0.647	4.35	9.46	7.96	7.98
4		0.0081	0.613	4.18	8.20	6.60	6.63
5		0.0071	0.609	3.72	6.93	5.77	5.79

II. TABULATED DATA FOR NITROGEN-MERCURY MIXTURE

Run Number	V_0 (ft/sec)	X	α	$\frac{V_g}{V_\ell}$	$V_g - V_\ell$ (ft/sec)	V_{0g} (ft/sec)	$\left(\frac{X}{1-X}\right)\left(\frac{\rho_\ell}{\rho_g}\right)$
I-1	0	-	0.138	-	-	0.28	-
2		-	0.111	-	-	0.22	-
3		-	0.101	-	-	0.19	-
4		-	0.085	-	-	0.15	-
5		-	0.062	-	-	0.085	-
6		-	0.105	-	-	0.21	-
7		-	0.083	-	-	0.16	-
8		-	0.241	-	-	0.86	-
9		-	0.239	-	-	0.72	-
10		-	0.176	-	-	0.51	-
11		-	0.094	-	-	0.23	-
12		-	0.308	-	-	0.93	-
13		-	0.247	-	-	0.82	-
14		-	0.224	-	-	0.71	-
15		-	0.197	-	-	0.49	-
16		-	0.332	-	-	1.19	-
17		-	0.317	-	-	1.11	-
18		-	0.267	-	-	0.95	-
19		-	0.381	-	-	1.30	-
20		-	0.341	-	-	1.03	-
21		-	0.296	-	-	0.86	-
22		-	0.270	-	-	0.63	-
23		-	0.206	-	-	0.39	-
J-1	0.10	0.000502	0.110	21.08	2.25	0.26	2.60
2		0.000469	0.117	18.26	1.96	0.24	2.42
3		0.000393	0.100	18.13	1.90	0.20	2.01
4		0.000290	0.080	16.70	1.71	0.15	1.45
5		0.000203	0.052	18.09	1.80	0.10	1.00
6		0.000144	0.039	17.15	1.68	0.07	0.70
7		0.001125	0.231	24.28	3.03	0.73	7.29
8		0.000944	0.185	23.30	2.73	0.53	5.29
9		0.00105	0.190	24.91	2.95	0.58	5.84

Run Number	V_0 (ft/sec)	X	α	$\frac{V_g}{V_\ell}$	$V_g - V_\ell$ (ft/sec)	V_{0g} (ft/sec)	$\left(\frac{X}{1-X}\right)\left(\frac{\rho_\ell}{\rho_g}\right)$
J-10	0.10	0.000670	0.134	23.34	2.58	0.36	3.61
11		0.00129	0.242	23.41	2.96	0.74	7.48
12		0.00150	0.256	26.15	3.38	0.90	9.00
13		0.00164	0.298	23.70	3.23	1.00	10.05
14		0.00183	0.321	24.60	3.48	1.16	11.64
15		0.00193	0.340	24.00	3.49	1.24	12.37
16		0.00114	0.225	22.14	2.73	0.64	6.43
17		0.00177	0.317	24.07	3.38	1.13	11.17
18		0.00263	0.374	29.10	4.49	1.74	17.38
19		0.00320	0.455	27.48	4.86	2.29	22.94
20		0.00352	0.463	27.60	4.49	2.53	25.20
K-1	0.20	0.000264	0.116	10.51	2.16	0.28	1.38
2		0.000247	0.110	10.44	2.13	0.26	1.29
3		0.000220	0.096	10.62	2.13	0.23	1.13
4		0.000203	0.084	11.35	2.26	0.21	1.04
5		0.000165	0.079	9.74	1.90	0.17	0.84
6		0.000122	0.052	10.94	2.09	0.11	0.60
7		0.000079	0.035	10.53	1.98	0.08	0.38
8		0.000624	0.212	13.17	3.08	0.71	3.54
9		0.000542	0.165	15.57	3.49	0.62	3.08
10		0.000439	0.144	14.34	3.12	0.48	2.41
11		0.000331	0.108	14.37	3.00	0.35	1.74
12		0.000217	0.062	16.63	3.33	0.22	1.10
13		0.000637	0.213	13.45	3.16	0.73	3.64
14		0.000716	0.245	13.15	3.21	0.85	4.27
15		0.000870	0.269	14.81	3.77	1.10	5.45
16		0.000954	0.295	14.39	3.79	1.20	6.02
17		0.001020	0.320	14.00	3.81	1.32	6.59
18		0.001840	0.478	13.93	4.96	2.55	12.76
19		0.001520	0.410	15.16	4.81	2.10	10.54
20		0.001250	0.381	13.43	4.01	1.65	8.26
21		0.000868	0.287	12.59	3.26	1.06	5.07
22		0.000407	0.171	10.98	2.41	0.45	2.27
L-1	0.30	0.000170	0.103	7.64	2.22	0.26	0.88
2		0.000491	0.250	8.54	3.01	0.85	2.85
3		0.000481	0.210	10.15	3.52	0.74	2.73
4		0.000374	0.200	8.00	2.62	0.63	2.00
5		0.000325	0.181	8.07	2.60	0.54	1.79
6		0.000271	0.152	8.15	2.52	0.44	1.47
7		0.000221	0.128	7.86	2.37	0.35	1.15
8		0.000658	0.293	9.73	3.71	1.21	4.03
9		0.000587	0.277	9.26	3.43	1.08	3.55
10		0.000495	0.235	9.39	3.30	0.87	2.89
11		0.000430	0.216	8.92	3.03	0.74	2.46
12		0.000569	0.259	9.70	4.03	1.02	3.39
13		0.000832	0.363	9.73	4.11	1.66	5.54
14		0.001103	0.431	9.70	4.59	2.20	7.35
15		0.001265	0.443	11.03	5.41	2.63	8.77

Run Number	V_0 (ft/sec)	X	α	$\frac{V_g}{V_\ell}$	$V_g - V_\ell$ (ft/sec)	V_{0g} (ft/sec)	$\left(\frac{X}{1-X}\right)\left(\frac{\rho_\ell}{\rho_g}\right)$
M-1	0.40	0.000355	0.238	6.59	2.93	0.82	2.06
2		0.000325	0.205	7.17	3.18	0.75	1.88
3		0.000283	0.184	7.28	3.09	0.63	1.64
4		0.000228	0.156	6.69	2.69	0.49	1.24
5		0.000182	0.126	6.63	2.57	0.38	0.96
6		0.000107	0.100	4.76	1.67	0.21	0.53
7		0.000389	0.253	6.44	2.92	0.87	2.18
M-8	0.40	0.000363	0.236	6.86	3.07	0.85	2.12
9		0.000342	0.225	6.69	2.94	0.78	1.94
10		0.000351	0.212	7.51	3.31	0.81	2.02
11		0.000382	0.238	6.99	3.16	0.87	2.18
12		0.000437	0.259	7.37	3.16	1.03	2.58
13		0.000479	0.290	6.36	3.02	1.09	2.60
14		0.000507	0.304	7.06	3.49	1.23	3.09
15		0.000224	0.156	6.41	2.57	0.47	1.18
16		0.000447	0.271	7.01	3.30	1.04	2.61
17		0.000664	0.355	7.85	4.25	1.73	4.32
18		0.000759	0.400	7.41	4.28	1.93	4.94
N-1	0.60	0.000304	0.271	4.74	3.07	1.05	1.76
2		0.000278	0.223	5.61	3.57	0.97	1.61
3		0.000254	0.224	4.93	3.03	0.85	1.42
4		0.000230	0.192	5.30	3.21	0.76	1.26
5		0.000323	0.271	5.10	3.37	1.14	1.90
6		0.000217	0.211	4.40	2.59	0.71	1.18
7		0.000356	0.287	5.05	3.41	1.21	2.03
8		0.000435	0.314	5.55	3.99	1.52	2.54
9		0.000519	0.352	5.90	4.52	1.92	3.20
10		0.000578	0.384	5.90	4.79	2.21	3.68
O-1	0.80	0.000295	0.262	4.98	4.36	1.41	1.77
2		0.000312	0.282	4.90	4.37	1.54	1.93
3		0.000332	0.285	5.14	4.61	1.64	2.05
4		0.000376	0.322	4.96	4.69	1.88	2.36
5		0.000354	0.312	4.81	4.42	1.75	2.19
6		0.000397	0.347	4.68	4.49	1.99	2.49
7		0.000441	0.364	4.94	4.95	2.26	2.83
8		0.000441	0.365	4.42	4.31	2.13	2.54
9		0.000414	0.353	4.52	4.34	1.97	2.47
10		0.000373	0.347	4.21	3.91	1.79	2.24
11		0.000308	0.286	4.49	3.92	1.44	1.80
12		0.000234	0.251	3.91	3.10	1.05	1.31
P-1	1.0	0.000266	0.287	3.85	4.02	1.55	1.55
2		0.000301	0.333	3.62	3.90	1.79	1.81
3		0.000342	0.336	4.24	4.89	2.14	2.14
4		0.000323	0.325	4.00	4.48	1.92	1.92
5		0.000285	0.302	3.92	4.17	1.69	1.70
6		0.000271	0.302	3.70	3.90	1.60	1.60

III. TABULATED DATA FOR NITROGEN-FREON-113 MIXTURE

Run Number	V_0 (ft/sec)	ϕ	X	α	$\frac{V_g}{V_\ell}$	$V_g - V_\ell$ (ft/sec)	V_{0g} (ft/sec)	$\left(\frac{X}{1-X}\right)\left(\frac{\rho_\ell}{\rho_g}\right)$
Q-1	0.870	0.00	0.00402	0.620	3.18	5.02	4.54	5.20
		0.30	0.00610		3.70	6.20	5.27	6.04
		0.60	0.00853		4.35	7.68	6.18	7.10
		0.80	0.01039		4.89	8.89	6.93	7.98
		1.00	0.01248		5.53	10.33	7.82	9.03
Q-2	0.870	0.00	0.00518	0.662	3.42	6.24	5.84	6.70
		0.30	0.00755		3.91	7.49	6.66	7.67
		0.60	0.01026		4.52	9.02	7.66	8.85
		0.80	0.01230		5.00	10.23	8.47	9.80
		1.00	0.01456		5.57	11.65	9.40	10.90
Q-3	0.870	0.00	0.00449	0.603	3.77	6.05	4.97	5.73
		0.30	0.00632		4.25	7.09	5.59	6.45
		0.60	0.00838		4.82	8.32	6.33	7.33
		0.80	0.00991		5.27	9.29	6.91	8.01
		1.00	0.01158		5.79	10.40	7.58	8.80
Q-4	0.870	0.00	0.00302	0.516	3.55	4.56	3.28	3.78
		0.30	0.00413		3.95	5.27	3.64	4.21
		0.60	0.00537		4.42	6.11	4.07	4.72
		0.80	0.00628		4.79	6.76	4.41	5.11
		1.00	0.00726		5.20	7.49	4.78	5.55
R-1	0.360	0.00	0.00422	0.525	4.90	2.89	1.91	5.42
		0.30	0.00681		5.85	3.59	2.27	6.47
		0.60	0.00992		7.10	4.50	2.75	7.85
		0.80	0.01236		8.18	5.28	3.16	9.04
		1.00	0.01518		9.51	6.24	3.66	10.51
R-2	0.360	0.00	0.00356	0.464	5.21	2.76	1.58	4.51
		0.30	0.00554		6.11	3.34	1.86	5.29
		0.60	0.00787		7.28	4.09	2.20	6.30
		0.80	0.00966		8.25	4.72	2.49	7.14
		1.00	0.01170		9.42	5.47	2.84	8.16
R-3	0.360	0.00	0.00222	0.357	4.96	2.16	0.97	2.75
		0.30	0.00342		5.80	2.62	1.13	3.22
		0.60	0.00484		6.88	3.20	1.34	3.82
		0.80	0.00593		7.77	3.68	1.51	4.31
		1.00	0.00717		8.84	4.26	1.72	4.91

ACKNOWLEDGMENTS

I wish to gratefully acknowledge the aid, guidance and encouragement that Professor N. J. Palladino gave throughout the development of this work. I am also indebted to Dr. M. Petrick of the Reactor Engineering Division at the Argonne National Laboratory for his consultation and advice. Particular thanks are due to Messrs. M. Gats, J. O'Grady and E. Gunchin for their assistance in the construction and operation of the apparatus.

The experimental part of this thesis was carried out at the Argonne National Laboratory, under a program sponsored by the Associated Midwest Universities and Argonne National Laboratory.

NOMENCLATURE

A	Froude-number exponent in dimensionless correlation
A_g	Cross-sectional area occupied by the gas phase (ft^2)
A_ℓ	Cross-sectional area occupied by the liquid phase (ft^2)
A_p	Cross-sectional area of flow (ft^2)
B	Froude-number exponent in empirical relation
C	Compressibility factor in P = CRT
D	Diameter of test section (ft)
f	Fanning friction factor (dimensionless) or function
F	Driving force (lb_f)
Fr	Froude Number, V_0^2/gD (dimensionless)
G	Mass flow rate per unit area ($lb_m/sec\text{-}ft^2$)
g	Gravitational constant, 32.2 ft/sec^2
g_c	Conversion factor, 32.2 $lb_m\text{-}ft/lb_f\text{-}sec^2$
H	Length in direction of flow (ft)
L	Length (ft)
M	Mass (lb_m)
k_i	Exponent, k_1, k_2, k_3, . . .
P	Static pressure (lb_f/ft^2)
R	Martinelli-Nelson two-phase friction factor
SH	Specific humidity (dimensionless)
T	Time (sec)
V_g	Average linear velocity of the gas phase (ft/sec)
V_ℓ	Average linear velocity of the liquid phase (ft/sec)
V_0	Superficial liquid velocity (ft/sec)
V_{0g}	Superficial gas velocity (ft/sec)
V_{0m}	Superficial velocity of the mixture (ft/sec)
v	Volume (ft^3)
v	Specific volume (ft^3/lb_m)
W_g	Gas mass flow rate (lb_m/sec)
W_ℓ	Liquid mass flow rate (lb_m/sec)
W_t	Total mass flow rate (lb_m/sec)
X	Mixture quality (dimensionless)

Greek

α	Void fraction (dimensionless)
Δ	Difference
ρ	Density (lb_m/ft^3)
ρ_g	Gas density ($lb_m ft^3$)
ρ_ℓ	Liquid density (lb_m/ft^3)
μ_ℓ	Dynamic viscosity of the liquid ($lb_m/ft\text{-}sec$)
π	Product
σ	Surface tension (lb_f/ft or dynes/cm), or standard deviation (dimensionless)
ϕ	Relative humidity (per cent)

Subscripts

ac	Acceleration
FR	Freon
g	Gas phase
h	Hydrostatic head
i	Indicates a location, i = 1, 2, 3, . . .
ℓ	Liquid phase
m	Two-phase mixture
N_2	Nitrogen
o	Superficial
s	Partial
sat	Saturation
t	Total
tpf	Two-phase friction